# Appendix 2.4.12-C

# Groundwater Flow Model for the Victoria County Station Site, Texas

**(87 pages)**

## Subsection 2.4.12-C Table of Contents


| Section | Title | Page |
|---|---|---|
| 2.4.12-C-1 | Purpose | 2.4.12-C-1 |
| 2.4.12-C-2 | Assumptions | 2.4.12-C-2 |
| 2.4.12-C-3 | Summary of Available Data | 2.4.12-C-3 |
| 2.4.12-C-3.1 | Regional Overview | 2.4.12-C-3 |
| 2.4.12-C-3.2 | Site-Specific Information | 2.4.12-C-4 |
| 2.4.12-C-3.3 | Stratigraphic Data | 2.4.12-C-5 |
| 2.4.12-C-3.4 | Groundwater Level Measurements | 2.4.12-C-6 |
| 2.4.12-C-3.5 | Hydraulic Conductivity | 2.4.12-C-7 |
| 2.4.12-C-3.6 | Other Properties | 2.4.12-C-9 |
| 2.4.12-C-4 | Numerical Model | 2.4.12-C-9 |
| 2.4.12-C-4.1 | Model Grid | 2.4.12-C-10 |
| 2.4.12-C-4.2 | Boundary Conditions | 2.4.12-C-13 |
| 2.4.12-C-5 | Model Calibration | 2.4.12-C-19 |
| 2.4.12-C-5.1 | Calibration Criteria | 2.4.12-C-19 |
| 2.4.12-C-5.2 | Summary of Calibrated Model Results | 2.4.12-C-21 |
| 2.4.12-C-6 | Predictive Simulations | 2.4.12-C-23 |
| 2.4.12-C-6.1 | Cooling Basin Seepage | 2.4.12-C-24 |
| 2.4.12-C-6.2 | Power Block Area Construction Dewatering Effects | 2.4.12-C-26 |
| 2.4.12-C-6.3 | Accident Release Pathway | 2.4.12-C-27 |
| 2.4.12-C-7 | Results | 2.4.12-C-28 |
| 2.4.12-C-8 | References | 2.4.12-C-29 |

## Subsection 2.4.12-C List of Tables


| Number | Title |
|---|---|
| 2.4.12-C-1 | VCS Site Average Groundwater Level Elevations |
| 2.4.12-C-2 | TWDB Groundwater Levels Used to Prepare Regional Potentiometric Surface Map |
| 2.4.12-C-3 | Harmonic Mean Vertical Hydraulic Conductivity of Layer 11 |
| 2.4.12-C-4 | Hydraulic Conductivity Values |
| 2.4.12-C-5 | Porosity Values |
| 2.4.12-C-6 | Summary of Model Boundary Conditions |
| 2.4.12-C-7 | Comparison of Simulated and Measured Heads |
| 2.4.12-C-8 | Estimated Cooling Basin Seepage |
| 2.4.12-C-9 | Cooling Basin Seepage Sensitivity Analysis |
| 2.4.12-C-10 | Summary of Predictive Dewatering Simulations |
| 2.4.12-C-11 | Summary of Particle Tracking Analysis |

## Subsection 2.4.12-C List of Figures


| Number | Title |
|---|---|
| 2.4.12-C-1 | Regional Potentiometric Surface Map |
| 2.4.12-C-2 | Plan View of Model Grid |
| 2.4.12-C-3 | Cross-Section of Model Grid (Model Row 92) |
| 2.4.12-C-4 | Recharge Zones in Pre-Construction Model |
| 2.4.12-C-5 | Model Calibration Statistics |
| 2.4.12-C-6 | Mass Balance after Calibration |
| 2.4.12-C-7 | Simulated Potentiometric Surface in Upper Shallow Aquifer in Model Layer 4 |
| 2.4.12-C-8 | Simulated Potentiometric Surface in Lower Shallow Aquifer in Model Layer 6 |
| 2.4.12-C-9 | Simulated Potentiometric Surface in Deep Aquifer in Model Layer 8 |
| 2.4.12-C-10 | Simulated Potentiometric Surface in Deep Aquifer in Model Layer 10 |
| 2.4.12-C-11 | Model Layer 4 Calibration Residuals |
| 2.4.12-C-12 | Model Layer 6 Calibration Residuals |
| 2.4.12-C-13 | Model Layer 8 Calibration Residuals |
| 2.4.12-C-14 | Model Layer 10 Calibration Residuals |
| 2.4.12-C-15 | Evapotranspiration Zones in Post-Construction Model Layer 1 |
| 2.4.12-C-16 | Cooling Basin River Boundary Condition in Model Layer 1 |
| 2.4.12-C-17 | Recharge Boundary Conditions at the Cooling Basin and Power Block Area in Model Layer 1 |
| 2.4.12-C-18 | Cooling Basin River Boundary Flow Rates for Post-Construction |
| 2.4.12-C-19 | Kuy Creek Drain Boundary Flow Rates |
| 2.4.12-C-20 | Dry Kuy Creek Drain Boundary Flow Rates |
| 2.4.12-C-21 | Downgradient Drain Boundary Flow Rates |
| 2.4.12-C-22 | Black Bayou and Linn Lake River and Constant Head Boundary Flow Rates |
| 2.4.12-C-23 | San Antonio River Boundary Flow Rates |
| 2.4.12-C-24 | Guadalupe River Boundary Flow Rates |
| 2.4.12-C-25 | Victoria Barge Canal River Boundary Flow Rates |
| 2.4.12-C-26 | Simulated Post-Construction Potentiometric Surface at the Power Block Area in Layer 2 |
| 2.4.12-C-27 | Cross-Section of Model Grid (Model Row 95) Showing Heads in Power Block Area |
| 2.4.12-C-28 | Simulated Post-Construction Potentiometric Surface at the Cooling Basin In Layer 2 |
| 2.4.12-C-29 | Cooling Basin Seepage Rates for Sensitivity Cases |

**List of Figures (Cont.)**


| Number | Title |
|---|---|
| 2.4.12-C-30 | Simulated Potentiometric Surface for Dewatering Scenario 1 in Layer 6 |
| 2.4.12-C-31 | Cross-Section of Dewatering Scenario 1 (Row 95) |
| 2.4.12-C-32 | Simulated Potentiometric Surface for Dewatering Scenario 2 in Layer 6 |
| 2.4.12-C-33 | Cross-Section of Dewatering Scenario 2 (Row 95) |
| 2.4.12-C-34 | Particle Tracking Results for Accident Scenario 1 in Layer 6 |
| 2.4.12-C-35 | Cross-Section of Particle Tracking Results for Accident Scenario 1 (Row 95) |
| 2.4.12-C-36 | Particle Tracking Results for Accident Scenario 2 in Layer 6 |
| 2.4.12-C-37 | Particle Tracking Results for Accident Scenario 3 in Layer 6 |
| 2.4.12-C-38 | Particle Tracking Results for Accident Scenario 4 in Layer 6 |

### 2.4.12-C-1 Purpose

The VCS Groundwater Flow Model is prepared to evaluate potential impacts on the groundwater flow system from the construction and operation of the cooling basin. Four specific areas of impact were assessed:

- Seepage rate from the cooling basin into the site groundwater system.
- Post-construction groundwater level in the power block area.
- Plant construction dewatering.
- Postulated post-construction accidental release groundwater pathway, including the impact of cooling basin seepage.

The groundwater flow model is executed under the Visual MODFLOW version 4.3 environment developed by Schlumberger Water Services (Reference 2.4.12-C-1). The program consists of a series of pre- and post-processors that feed information to various numerical groundwater flow models developed by others. The groundwater flow model selected for the VCS utilizes a three-dimensional finite-difference groundwater flow model known as MODFLOW-2000 (Reference 2.4.12-C-2). This model consists of a main program that directs the execution of the simulation and a series of user selectable packages or modules that do the following:

1. Simulate groundwater flow using block-centered (BCF), hydrogeologic unit (HUF), or layer property (LPF) finite-difference approaches.
2. Control the solution of the finite-difference equations to represent the system (GMG, LMG [SAMG], PCG2, WHS, SIP1, or SOR1).
3. Simulate boundary conditions, including drains (DRN1), evapotranspiration (EVT1), general head boundaries (GHB1), horizontal flow barriers (HFB1), lakes (LAK3), recharge (RCH1), rivers (RIV1), specified head boundaries (CHD1), streams (STR1), and wells (WEL1).

Additionally, a subsidiary program known as MODPATH (Reference 2.4.12-C-3) is used to perform particle tracking to estimate travel time from postulated radwaste buildings within the power block to the nearest receptor for simulation of the accidental release groundwater pathways for radionuclides.This work was accomplished by the following processes (Reference 2.4.12-C-4):

- Develop a conceptual hydrogeologic model
- Develop groundwater flow model design
- Calibrate numerical model using existing data

- Perform a sensitivity analysis to document the effects of parameter uncertainty
- Perform predictive simulations
- Perform a sensitivity analysis to document the effects of uncertainty in predictive simulations
- Document modeling results

Note that all references to elevations given in this appendix are to the North American Vertical Datum of 1988 (NAVD 88), unless otherwise indicated.

### 2.4.12-C-2 Assumptions

The general assumptions used in the model include:

- Homogeneous conditions are assumed for each material type (sand or clay).
- The flow regime represents a constant density system.
- The flow regime represents an equivalent porous medium based on the granular nature of the materials.
- A single value of hydraulic conductivity is selected for each of the sand units represented in the model.
- For the pre-construction conditions, two zones of recharge are assumed for the model area: Zone 1 represents the uplands, where clay is the dominant surficial material and Zone 2 represents the surface outcrop of sand units, where recharge is interpreted to be higher.
- Review of the Texas Water Development Board (TWDB) well logs and reports suggests that there are no major groundwater extraction areas within the model area. The majority of wells within the model area are domestic, stock watering, and oil and gas rig water supply wells. These types of wells are assumed to have average pumping rates of less than 10 gpm, which would have minimal impact on groundwater levels outside of the immediate area of the well. Therefore, with the exception of the accident analysis particle tracking, pumping from individual wells is not included in the model.
- Simulations are assumed to represent steady-state conditions, since there is little evidence to suggest that time-dependent (transient analysis) is necessary, nor is there sufficient onsite or offsite historical groundwater level data to support transient modeling.

Upon plant completion, the following cooling basin/power block area parameters are assumed:

- The hydraulic conductivity ($K_h$) of the fill material used in plant construction is assumed to be that of a clean sand and gravel at 500 feet/day (Reference 2.4.12-C-4). A $K_h/K_v$ of 10 was used for the backfill to represent the vertical anisotropy created by compaction of lifts of the fill material.

- Samples of proposed structural fill were obtained from local, offsite suppliers, and particle size distributions were determined by sieve analysis as reported in Part 5 of the ESPA. Hydraulic conductivity of the proposed backfill was determined using the mean grain size and the Shepherd equation (Reference 2.4.12-C-18). Using the Shepherd equation for texturally immature (poorly sorted, angular) consolidated sediments, the estimated hydraulic conductivities for the three samples that most closely approximate the preferred structural fill for the VCS site (sample numbers Fordyce Briggs RAW, CWA #4 and CWA #6) are 163 feet/day, 1013 feet/day, and 732 feet/day, respectively. The geometric mean of these three values is 495 feet/day, which substantiates the value assumed in the numerical model for the horizontal hydraulic conductivity of structural fill (500 ft/day).

- Post-construction recharge is represented by: no recharge in the cooling basin and power block building areas, twice the pre-construction Zone 2 recharge is assumed in power block backfill areas, and the pre-construction recharge distribution is assumed for all other model areas. The power block area backfill is assumed to be approximately five times more permeable than the natural sand units, however mitigating surface features such as finish grading to assure overland flow rather than ponding, storm drains to conduct surface drainage, and vegetation control are assumed to reduce the amount of infiltration through the backfill.

- The VCS cooling basin bottom is assumed to be elevation 69 feet.

- The cooling basin dikes are not considered in the seepage analysis due to their small size in relation to the cooling basin area.

- The power block is assumed to be excavated to elevation -15 feet.

- The level for the VCS cooling basin is assumed to be elevation 90.5 feet ± 1 foot.

- The finished plant grade in the power block area is assumed to be elevation 95 feet.

### 2.4.12-C-3 Summary of Available Data

#### 2.4.12-C-3.1 Regional Overview

The VCS site is located in southern Victoria County and is approximately 13.3 miles south of the City of Victoria, Texas. The VCS site lies within the Coastal Prairies subprovince of the Gulf Coastal

Plains physiographic province, which extends as a broad band along the coast of the Gulf of Mexico. The geologic materials underlying the Coastal Prairies subprovince is that of a deltaic depositional environment. This deltaic environment consists of a complex overlapping series of braided stream, levee, lagoon, and overbank flood sediments deposited in the Gulf of Mexico Basin during the Pleistocene. The deltaic depositional environment was influenced by a series of transgressive and regressive sea levels in the Gulf of Mexico (Reference 2.4.12-C-5). The deltaic depositional environment would be similar to that seen on the present-day Mississippi delta. In the subsurface, deltaic deposits appear as alternating and interfingering layers of clay, sand, gravel, and silt. Continental uplift and subsidence of underlying sediments within the Gulf of Mexico Basin have produced units that dip toward the Gulf of Mexico.

The primary aquifers in the site area are the Chicot and Evangeline aquifers. The Chicot aquifer is comprised of the Pleistocene-aged Beaumont Clay and the Lisse Formation. Defining a stratigraphic contact between these formations is problematic due to the considerable heterogeneity of the sediments, a general absence of index fossils and marker beds, and an absence of diagnostic electric log signatures. The Evangeline aquifer is comprised primarily of the Pliocene-aged Goliad Sand, which consists of coarse-grained sediments. The Chicot and Evangeline aquifers are components of the encompassing Gulf Coast aquifer system, which is the primary aquifer system along the Gulf Coast of Texas (Reference 2.4.12-C-5).

### 2.4.12-C-3.2 Site-Specific Information

The VCS site is a greenfield site and little historical hydrogeologic data are available. The site consists of approximately 11,500 acres of land presently used for cattle ranching, oil and gas production, and recreational uses. The proposed site land utilization includes areas for the power block, the cooling basin, and support facilities. Figure 2.4.12-3 of Subsection 2.4.12 presents a plan view of the proposed VCS layout.

Plant-specific subsurface information for the VCS site was obtained primarily from the site investigation program conducted between September 2007 and February 2008 as described in Subsections 2.4.12.1.4 and 2.5.4. The subsurface investigation consisted of geotechnical borings logs, borehole geophysics, geotechnical field and laboratory testing, cone penetrometers, installation of groundwater observation wells, performance of slug tests and pumping tests, and other geotechnical and hydrogeologic data collection.

The power block area of the site is presently at an approximate elevation of 80 feet and the ground surface is generally flat within the power block area. Plant-specific boring information suggests that the bottom of the Chicot aquifer is approximately 300 feet below current ground surface in the power block area. To the east of the power block area, a steep decrease in surface elevation marks the edge of the Guadalupe River Valley. The surface elevation on the Guadalupe River floodplain is

approximately 15 feet. It should be noted that site elevations are reported referencing the NAVD 88 elevation datum, while the elevations on some of the regional maps used as background are referenced to the National Geodetic Vertical Datum of 1929 (NGVD 29). The datum shift between NAVD 88 and NGVD 29 is approximately 0.44 feet in the VCS area (Reference 2.4.12-C-6).

The Chicot aquifer is subdivided into three saturated sandy zones at the VCS site: the “Upper Shallow” aquifer, the “Lower Shallow” aquifer, and the “Deep” aquifer. Additionally, a sand layer designated the “Sand 1” aquifer exists above the saturated zone beneath the cooling basin. These sand units are separated by less permeable layers of clayey materials. The primary zones of concern for VCS cooling basin seepage and excavation dewatering are the Sand 1 aquifer and the Upper Shallow aquifer.

### 2.4.12-C-3.3 Stratigraphic Data

Site investigation borehole log data and borehole geophysical logs were combined with offsite TWDB driller’s logs (Reference 2.4.12-C-7) to develop a stratigraphic model of the area. Geologic cross-sections were prepared to correlate the onsite geotechnical layering information to the TWDB driller’s logs representing the regional stratigraphy. The stratigraphic interpretations were used to create kriged surfaces for each layer, which were imported into the model grid as the bottom elevation of each model layer. Where a layer was missing, a thickness of 1 foot was assigned to the layer, and the properties of the underlying layer were used.

Eleven model layers were chosen to represent the component of the Chicot Aquifer based on the borehole data. The model layers representing the sand layers at the VCS site are: Unsaturated Sand or Sand 1 (model layer 2), Upper Shallow aquifer or Sand 2 (model layer 4), Lower Shallow aquifer or Sand 4 (model layer 6), and the Deep aquifer representative of Sand 5 and Sand 6 (model layers 8 and 10). The interfingering clay layers (Clay 1 Top, Clay 1 Bottom, Clay 3, Clay 5 Top, and Clay 5 Bottom) are represented by model layers 1, 3, 5, 7, 9. Model layer 11 encompasses Clay 7, Sand 8, Clay 9, and Sand 10. The explicit method of representing a confining layer using a model layer was selected to represent the confining layers at the VCS site, resulting in the following eleven model layers:

**Relative Frequency of Detection in Site Boreholes**

ya6 ra6 Ga6 ta6 ca6 ha6 na6 ia6 Ha6 yaa6

| Model Layer | Geotechnical Layer | Hydrogeologic Unit |
|---|---|---|
| Layer 1 | Clay 1 Top | |
| Layer 2 | Sand 1 | Unsaturated Sand Layer |
| Layer 3 | Clay 1 Bottom | |
| Layer 4 | Sand 2 | Upper Shallow Aquifer |
| Layer 5 | Clay 3 | |
| Layer 6 | Sand 4 | Lower Shallow Aquifer |
| Layer 7 | Clay 5 Top | |
| Layer 8 | Sand 5 | Deep Aquifer |
| Layer 9 | Clay 5 Bottom | |
| Layer 10 | Sand 6 | Deep Aquifer |
| Layer 11 | Clay 7, Sand 8, Clay 9, Sand 10 | |

The relative frequencies of detection of the units indicate continuity or lack thereof for each geotechnical layer.

### 2.4.12-C-3.4 Groundwater Level Measurements

Because the VCS site is a greenfield site, little historical groundwater level data exist for the site proper, however the TWDB does maintain several observation wells close to the site to measure water levels in the Chicot and Evangeline aquifers. Regionally, groundwater flow is generally toward the southeast, or toward the Gulf of Mexico, as shown in Figure 2.4.12-13 in Subsection 2.4.12, which is a regional potentiometric surface map for the Chicot aquifer for 1999. The limited number of data points in the site area would obscure any localized impacts from rivers in the site area. Figure 2.4.12-14 in Subsection 2.4.12 presents the steady-state simulated groundwater level elevations in the Chicot aquifer using the calibrated Central Gulf Coast Groundwater Availability Model (GAM) (Reference 2.4.12-C-8). This map shows the influence of the Guadalupe and San Antonio rivers on localized flow conditions adjacent to the site, where an east-west component of flow is overlain on the regional flow pattern.

Monthly groundwater level measurements commenced at the site in October of 2007 through February 2009. Quarterly measurements commenced after February 2009. Table 2.4.12-C-1 presents the arithmetic mean value of the VCS site groundwater levels collected through August 2009. Potentiometric surface maps for VCS site groundwater level measurements are presented in Subsection 2.4.12, Figure 2.4.12-15. These values along with groundwater level measurements for three TWDB observation wells were used as calibration targets for the groundwater model. Water level measurements from the TWDB observation wells were averaged over the years 2007 through 2009 to provide a comparable dataset to site observations.

A regional potentiometric surface was developed using groundwater levels from selected TWDB well logs. The general regional flow pattern shown in Figure 2.4.12-14 in Subsection 2.4.12 and the site-specific measurements were used to identify anomalies in the well log water levels. These anomalies were removed along with densely clustered data. Considering the dense coverage of available driller's logs across the model domain and the fact that the data was collected over a period of 20 years, censoring a portion of the dataset is not believed to significantly skew the results. Table 2.4.12-C-2 presents the groundwater level data selected for use. The resulting potentiometric surface is shown in Figure 2.4.12-C-1. This figure was created using linear kriging with a 500 feet by 500 feet grid. Because this figure is based on measurements not synoptically collected, the resulting potentiometric surface is assumed to represent average conditions in the aquifers, which is appropriate for steady-state analysis. The wells used to prepare this map are primarily screened in the Deep aquifer although some wells are screened in the Upper and Lower Shallow aquifers. Therefore, the potentiometric surface shown in Figure 2.4.12-C-1 generally represents conditions in the Deep aquifer. Based on the VCS site groundwater level measurements, the vertical head

differential between the different aquifer units within the Chicot Aquifer is small relative to the horizontal hydraulic gradient across the site and therefore, it is reasonable to project this relationship to that of the Upper Shallow and Lower Shallow aquifers and across the larger area covered by the map.

### 2.4.12-C-3.5 Hydraulic Conductivity

A variety of hydraulic conductivity values were needed to support defining the groundwater flow system. The following list summarizes the data needs and methodology for determining the values:

- Horizontal hydraulic conductivity of the Upper Shallow aquifer (Sand 2) represents the value determined from a 48-hour aquifer pumping test performed in test well TW-2320U in this unit as shown in Subsection 2.4.12, Table 2.4.12-9.

- Horizontal hydraulic conductivity of the remaining saturated sand layers, including the Lower Shallow aquifer (Sand 4) and Deep aquifer (Sand 5 and Sand 6), represents the hydraulic conductivity derived from a 24-hour aquifer pumping test performed in test well TW-2359L in Sand 5 as shown in Subsection 2.4.12, Table 2.4.12-9. The horizontal hydraulic conductivities of Sand 4, Sand 5, and Sand 6 are assumed to be equal, based upon grain size analysis, as shown in Subsection 2.4.12, Figure 2.4.12-22.

- Vertical hydraulic conductivity of the sand layers was calculated using the typical ratio of Kh/Kv = 3 (Reference 2.4.12-C-9).

- Vertical hydraulic conductivity of layer 1 of the model (Clay 1) was assigned a Kv representing the maximum hydraulic conductivity determined from borehole permeameter tests (Subsection 2.4.12, Table 2.4.12-14) and the remaining clay layers were assigned a Kv based on laboratory permeability testing of undisturbed soil samples from Subsection 2.4.12, Table 2.4.12-13.

  The values of vertical hydraulic conductivity selected for the modeled clay layers are conservative with respect to both cooling basin seepage and groundwater mounding at the power block. The value selected for the vertical hydraulic conductivity of the uppermost model layer (layer 1, Clay 1), 0.068 feet/day, is the maximum value measured by the Guelph Permeameter testing of this layer. This value provides a conservative analysis with respect to groundwater mounding at the power block because it allows the highest plausible rate of seepage from the cooling basin and prediction of correspondingly high groundwater levels in the power block.

  The base of the cooling basin will be exposed to both the surface clay layer (model layer 1) and Sand 1 (model layer 2). Seepage through Sand 1 will be confined by an underlying shallow clay layer (model layer 3). This shallow confining clay layer has been assigned a vertical hydraulic

conductivity of 7 x $10^{-5}$ feet/day, as have the deeper confining layers in the model. Selecting a value of vertical hydraulic conductivity greater than that used in the VCS model for the shallow and deeper confining clay layers would result in lowering of the groundwater head at the power block. This would result because more seepage would occur through the shallow confining clay layer into the underlying Upper Shallow aquifer (Sand 2), where the regional hydraulic gradient would induce groundwater flow toward the east. The 7 x $10^{-5}$ feet/day value of vertical hydraulic conductivity is the geometric mean of five values determined by laboratory testing of undisturbed soil samples from the Shallow and Deep Confining Layers (Subsection 2.4.12, Table 2.4.12-13) and is considered representative for these clay layers.

The value (0.068 feet/day) for the vertical hydraulic conductivity of layer 1 (surface clay layer) in the VCS model is greater than the highest value reported in Reference 2.4.12-C-17 for the vertical hydraulic conductivity of the clay units in the Chicot aquifer [4.63 x $10^{-4}$ meter/day (1.52 x $10^{-3}$ feet/day) to 0.73 x $10^{-5}$ meter/day (2.4 x $10^{-5}$ feet/day)]. The value 7 x $10^{-5}$ feet/day is at the low end of the range reported in Reference 2.4.12-C-17 for the vertical hydraulic conductivity of the deeper clay units in the Chicot Aquifer. On this basis, use of a higher value for layer 1 or a lower value for the deeper clay layers in the VCS model is not justified.

It can be noted that during the pumping test completed in the Deep aquifer, groundwater levels were monitored in an observation well completed in the Lower Shallow aquifer. The results of that test indicate that there was no water-level response in the Lower Shallow aquifer resulting from pumping of the Deep aquifer. Therefore, it can be concluded that the Lower Shallow and Deep aquifers are hydraulically isolated in the area of the test. This finding supports the use of a relatively low value (i.e., 7 x $10^{-5}$ feet/day) for the vertical hydraulic conductivity of the confining clay layers in the VCS groundwater model.

- Horizontal hydraulic conductivity of clayey layers – used the relationship Kh/Kv = 10 (Reference 2.4.12-C-9), a higher anisotropy ratio was used for the clays due to the presence of sand layers interbedded with the clay.

- Layer 11 was considered a special case because it includes both sand and clay layers. The vertical hydraulic conductivity of this layer is the weighted harmonic mean of the sand and clay layers as shown on Table 2.4.12-C-3, which includes the thickness and hydraulic conductivity for each unit. The relationship Kh/Kv = 10 was used to estimate the horizontal hydraulic conductivity.

- Vertical hydraulic conductivity of cooling basin bottom material (Sand 1) – maximum hydraulic conductivity from tests measuring saturated hydraulic conductivity of sand are discussed in Subsection 2.4.12.2.4.2 and Table 2.4.12-14.

The hydraulic conductivity values used in the model are summarized in Table 2.4.12-C-4. Some of the hydraulic conductivity values were adjusted as part of model calibration to match the observed heads.

### 2.4.12-C-3.6 Other Properties

Other properties used to support model development include recharge rate, evapotranspiration, specific storage, specific yield, and porosity. Values for these properties were established as described below.

The recharge rate was treated as a calibration parameter. The GAM (Reference 2.4.12-C-8) indicates a recharge rate range from 0.09 to 0.43 inches/year [$2 \times 10^{-5}$ to $9.8 \times 10^{-5}$ feet/day] for the northern and southern Gulf Coast GAMs. The recharge rate was varied within this range during calibration to obtain the best match to observed groundwater levels at the site. Model calibration using recharge is discussed in more detail in Subsection 2.4.12-C-5.

The evapotranspiration (ET) rate in the upland areas (including the VCS site) is negligible because groundwater levels are greater than 30 feet below ground surface; however, in the Guadalupe and lower San Antonio River valleys groundwater levels are at or near the ground surface. ET data as potential evapotranspiration (PET) has been calculated for Victoria County (Reference 2.4.12-C-10). The average PET rate is 57.02 inches/year with an average precipitation of 39.17 inches/year. In addition to the PET rate, an extinction depth is also needed to represent ET in the model. The extinction depth typically represents the maximum depth of the root zone. For the site area, an extinction depth of 5 feet is assumed.

The arithmetic mean total and effective porosity for each model layer are presented in Table 2.4.12-C-5. The specific yield of the different geotechnical layers is assumed to be the same as the effective porosity (Reference 2.4.12-C-9). The specific storage of the geotechnical layers was estimated using the mean storage coefficient from the TW-2320U aquifer pumping test ($1.84 \times 10^{-5}$) and the saturated thickness of 7 feet (Subsection 2.4.12, Table 2.4.12-9). The resultant specific storage is $2.63 \times 10^{-6}$ $feet^{-1}$. It should be noted that specific yield and specific storage are not needed for steady-state simulations, but are included in the Visual MODFLOW input for completeness.

### 2.4.12-C-4 Numerical Model

The model area was established to take advantage of natural boundary conditions in the site area. The Guadalupe and San Antonio Rivers, the Victoria Barge Canal, and Coleto Creek form physical boundaries along the north, east, west, and south perimeters of the model domain. Groundwater flow directions are interpreted as generally west to east across the VCS site, based on the regional potentiometric surface presented in Figure 2.4.12-C-1. Pre-construction groundwater discharge is interpreted to occur on the west side of the Guadalupe River valley into Linn Lake and a series of

sloughs that run along the west side of the valley by discharge into these surface water features and by ET.

### 2.4.12-C-4.1 Model Grid

The model grid consists of 189 columns, 193 rows, and 11 layers. Grid spacing ranges from 500 feet at the edges to 250 feet in the power block area. Figure 2.4.12-C-2 is a plan view of the model domain showing the grid and calibration wells. Figure 2.4.12-C-3 shows a west to east cross-section through the model, passing through the proposed power block area.

The initial heads used in the model were determined in two steps. First, the heads were arbitrarily set to elevation 100 feet in each layer. A small value of ET (0.57 inch/year) was used in the initial simulation, and the resulting head distribution was saved at the end of the simulation. The ET rate was gradually increased to a realistic ET value of 57.02 inches/year.

Surface topography was incorporated into the model using the U.S. Geological Survey's National Elevation Dataset (NED) (Reference 2.4.12-C-11). This dataset has surface elevations referenced to the NAVD 88 vertical datum.

A layer type is defined for each layer in the model. The layer type represents the hydrogeologic conditions anticipated for each layer. For the VCS pre-construction model the layer type for all layers was Type 3 – Confined/Unconfined, with variable storage coefficient and transmissivity. The following layer definitions are used:

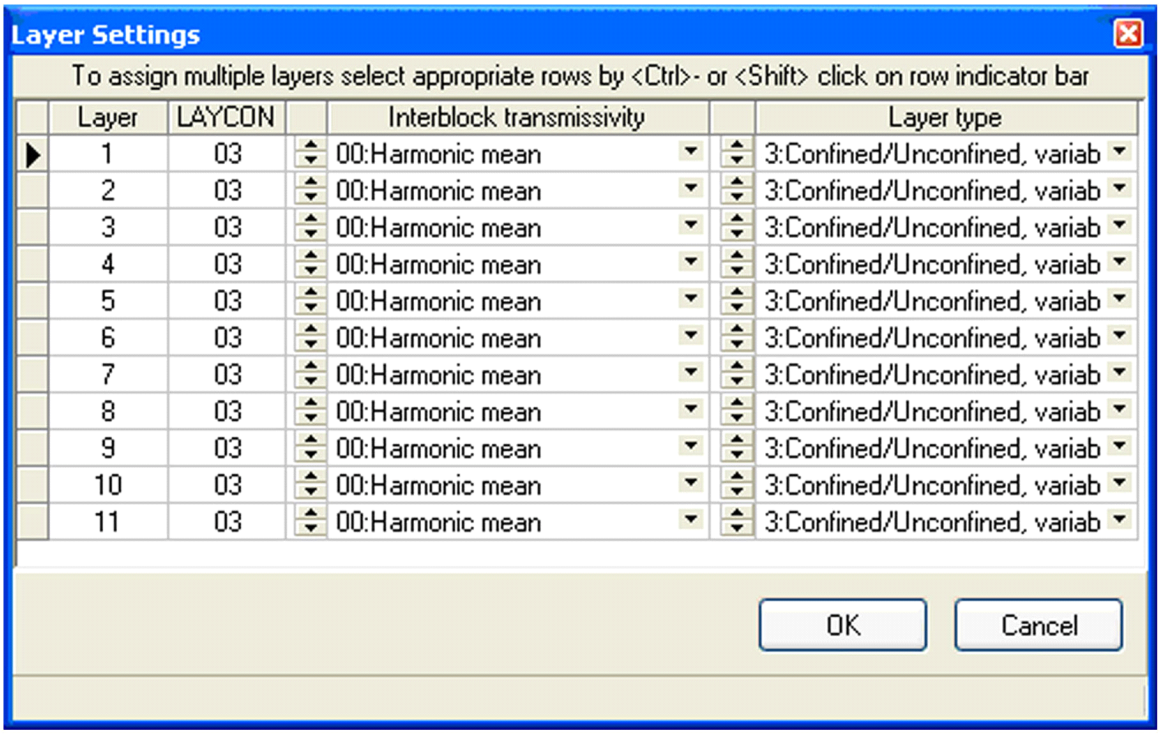


The MODFLOW default method for assigning inter-block transmissivity using the harmonic mean is used for all layers.

The solver used in the model is the algebraic multigrid (SAMG) solver (Reference 2.4.12-C-12). The following settings were used in the solver:

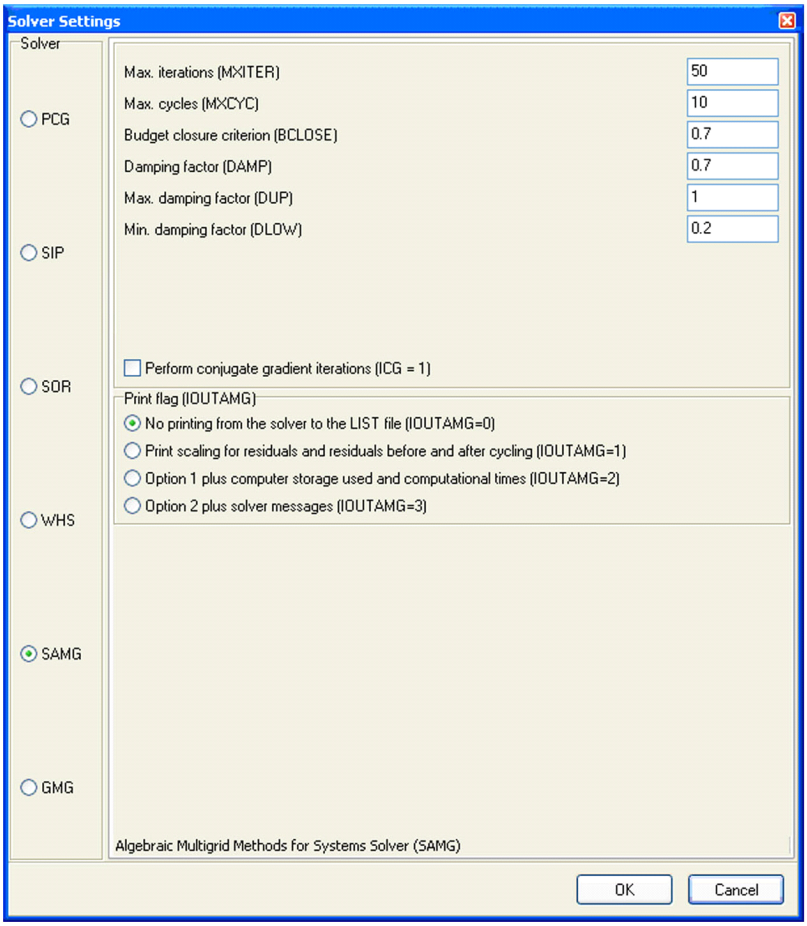


The SAMG solver has advantages over other solvers included with Visual MODFLOW for problems with large grids or a highly variable hydraulic conductivity field. The solver is also less sensitive to the initial head distribution (Reference 2.4.12-C-1).

The configuration of the model requires the use of the re-wetting function to saturate unsaturated cells in the model. The following settings were used:

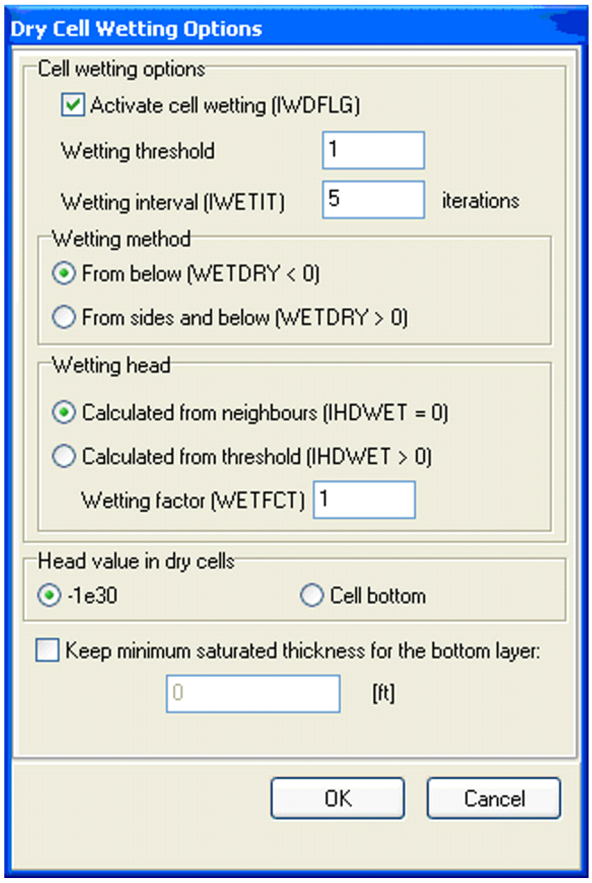


The discontinuity of the strata in the top four layers of model produces cyclic wetting and drying of cells in the areas where steep changes in layer elevations and stratigraphic layer pinch outs occur. This cyclic wetting and drying interferes with numerical convergence by the solver. By increasing the wetting interval, the solver can converge on a solution. A recommended range for the wetting interval is between three and five iterations (Reference 2.4.12-C-13)

### 2.4.12-C-4.2 Boundary Conditions

The pre-construction model boundary conditions are summarized in Table 2.4.12-C-6. The following boundaries were used in the groundwater flow model:

**Recharge**

The recharge boundary condition was assigned to the uppermost active model cell. Two zones of recharge were used for pre-construction conditions - Zone 1 represents areas overlain by clay and was initially assigned a value of 0.2 inch/year and Zone 2 represents areas overlain by sandy

deposits and was initially assigned a value of 0.4 inch/year. These values were adjusted during calibration. The recharge zones used in the model are presented in Figure 2.4.12-C-4.

**Evapotranspiration**

The ET boundary condition was assigned as a single zone. The zone was assigned an ET of 57.02 inches/year throughout the model domain. An extinction depth of 5 feet was used to represent the maximum root penetration depth. It should be noted that Visual MODFLOW stops ET if the groundwater level is below the extinction depth or below the bottom of layer 1. Over most of the valley areas, layer 1 is 1 foot thick. To overcome this restriction, the thickness of layer 1 was increased to 5 feet in the valley areas. Although this represents a deviation from the conceptual model, the overall transmissivity relationship of the layers remains unchanged because layer 1 is assigned the hydraulic conductivity of the underlying unit.

**General Head**

The general head boundaries were assigned using a boundary distance of 10,000 feet, a hydraulic gradient for the west side of the model of 0.0012 feet/feet, a hydraulic gradient for the northeast and east sides of the model of 0.008 feet/feet (Figure 2.4.12-C-1), and the head distribution from Figure 2.4.12-C-1. The head at the boundary was computed by multiplying the boundary distance (10,000 feet) by the hydraulic gradient (0.0012 feet/feet or 0.008 feet/feet) to obtain a value of 12 feet or 8 feet. These values were added to the head measurements at the appropriate edge of Figure 2.4.12-C-1 to obtain the head at the boundary.

Layer 4 – Along the west edge of the model grid to represent regional inflow of groundwater in the Upper Shallow aquifer. The head elevations for the boundary were assigned using a linear gradient ranging from 92 to 72 feet (north to south). A hydraulic conductivity of 68 feet/day and an east-west face for applying the boundary were used. Along the northeast edge of the model to represent regional inflow from the north. The head elevation for the boundary was assigned as 38 feet, with a hydraulic conductivity of 68 feet/day and a north-south face for applying the boundary.

Layer 6 – Along the west side of the model grid to represent regional groundwater inflow in the Lower Shallow aquifer. The head elevations for the boundary were assigned using a linear gradient ranging from 92 to 72 feet (north to south). A hydraulic conductivity of 103 feet/day and an east-west face for applying the boundary were used. Along the northeast and east sides of the model to represent regional groundwater inflow. The head elevations were assigned using a uniform 38 feet in the northeast and a linear gradient ranging from 38 to 13 feet along the east side, a hydraulic conductivity of 103 feet/day, and either a north-south face for the northeast or an east-west face for the east sides of the model.

Layer 7 – Along the southern portion of the east side of the model grid to represent outflow in the sand portion of this layer. The head elevation was assigned as a linear gradient ranging from 23 to 16 feet, with a hydraulic conductivity of 103 feet/day and an east-west face for applying the boundary.

Layer 8 – Along the west side of the model grid to represent regional groundwater inflow in the Deep aquifer. The head elevations for the boundary were assigned using a gradient fill ranging from 92 to 72 feet (north to south). A hydraulic conductivity of 103 feet/day and an east-west face for applying the boundary were used. A second general head boundary was assigned along the northeast and east edges of the model domain to represent groundwater outflow in the Deep aquifer. The head elevations were assigned using a uniform 38 feet in the northeast and a linear gradient ranging from 38 to 13 feet along the east side, a hydraulic conductivity of 103 feet/day, and either a north-south face for the northeast or an east-west face for the east sides of the model.

Layer 9 – Along the southern portion of the east side of the model grid to represent outflow in the sand portion of this layer. The head elevation was assigned as a linear gradient ranging from 23 to 16 feet, with a hydraulic conductivity of 103 feet/day and an east-west face for applying the boundary.

Layer 10 – Along the west side of the model grid to represent regional groundwater inflow in the Deep aquifer. The head elevations for the boundary were assigned using a linear gradient ranging from 92 to 72 feet (north to south). A hydraulic conductivity of 103 feet/day and an east-west face for applying the boundary were used. A second general head boundary was assigned along the northeast and east edges of the model domain to represent groundwater outflow in the Deep aquifer. The head elevations were assigned using a uniform 38 feet in the northeast and a linear gradient ranging from 38 to 13 feet along the east side, a hydraulic conductivity of 103 feet/day, and either a north-south face for the northeast or an east-west face for the east sides of the model.

**Drain**

Layer 1 – Drain boundaries were assigned along Kuy and Dry Kuy Creeks, other unnamed creeks adjacent to the VCS site, and on the Guadalupe River Valley slope to the east of the proposed cooling basin to simulate seepage areas in the clay layer (Clay 1T). The unnamed creeks and the Guadalupe River Valley seeps are lumped together and referred to as “the downgradient drains.” The drain elevations were assigned using a Visual MODFLOW formula ($BOT + 1.0), which places the drain elevation at 1 foot above the bottom of the cell.

Layer 2 – Drain boundaries were assigned along Kuy and Dry Kuy Creeks, other unnamed creeks adjacent to the VCS site, and on the Guadalupe River Valley slope to the east of the proposed cooling basin to simulate seepage areas in the layer (Sand 1). The unnamed creeks and the Guadalupe River Valley seeps are lumped together and referred to as “the downgradient drains.” The drain elevations were assigned using a Visual MODFLOW formula ($BOT + 1.0), which places the drain elevation at 1 foot above the bottom of the cell.

Layer 3 – Drain boundaries were assigned along Kuy Creek from its confluence with Dry Kuy Creek to its confluence with the Guadalupe River to simulate seepage from Clay 1B, which is exposed in this area. The drain elevations were assigned using a Visual MODFLOW formula ($BOT + 1.0), which places the drain elevation at 1 foot above the bottom of the cell.

Two types of conductance values were used for the drains: drains present at the bottom of drainage channels and drains present in the sides of drainage channels. The definition of conductance for drains in the bottom of drainage channels is based on a 2 feet thick sediment layer (*M*) with a vertical hydraulic conductivity of 2.75 feet/day (*K*) (based on Sand 1 testing [Subsection 2.4.12, Table 2.4.12-14]). For Kuy Creek (west of the confluence with Dry Kuy Creek) and Dry Kuy Creek in model layer 2, a drain width of 20 feet (*W*) and a length of 500 feet (*L*) is assumed. The conductance (*C*) for an open drain is then (Reference 2.4.12-C-4):

$$C = \frac{KLW}{M} = \frac{2.75 \times 500 \times 20}{2} = 13750\ ft^2\ /\ day$$

The conductance (*C*) per unit length (*L*) would be:

$$C/L = \frac{13750}{500} = 27.5\ ft\ /\ day$$

For the downgradient drains east of the cooling basin in model layer 2, the same vertical hydraulic conductivity, drain length, and thickness are assumed with a drain width (*W*) of 500 feet:

$$C = \frac{2.75 \times 500 \times 500}{2} = 343750\ ft^2\ /\ day$$

And a conductance (*C*) per unit length (*L*) of:

$$C/L = \frac{343750}{500} = 688\ ft\ /\ day$$

For the downgradient drains north of the VCS (unnamed tributaries) the conductance values for Kuy Creek are used.

For drains in model layer 1 and in Kuy Creek east of the confluence with Dry Kuy Creek in model layer 2, the drains are present on the banks of the drainage channel and the conductance is based on a 1 foot thick sediment layer (*M*) with a vertical hydraulic conductivity of 2.75 feet/day (*K*) [based on Sand 1 testing (Subsection 2.4.12, Table 2.4.12-14)]. The drain width is the saturated thickness of

the drain cell, which is defined by Visual MODFLOW as $\$\Delta Z$, the conductance per unit length (*L*) would be:

$$C/L = 2 \times \frac{2.75 \times \$\Delta Z}{1}$$

The conductance per unit length values are doubled because the drains would be present on both sides of the channel.

$$C = \frac{KLW}{M} = \frac{2.75 \times 500 \times 20}{2} = 13750\ ft^2\ /\ day$$

The conductance (*C*) per unit length (*L*) would be:

$$C/L = \frac{13750}{500} = 27.5\ ft\ /\ day$$

For the downgradient drains east of the cooling basin in model layer 2, the same vertical hydraulic conductivity, drain length, and thickness are assumed with a drain width (*W*) of 500 feet:

$$C = \frac{2.75 \times 500 \times 500}{2} = 343750\ ft^2\ /\ day$$

And a conductance (*C*) per unit length (*L*) of:

$$C/L = \frac{343750}{500} = 688\ ft\ /\ day$$

For the downgradient drains north of the VCS (unnamed tributaries) the conductance values for Kuy Creek are used.

For drains in model layer 1 and in Kuy Creek east of the confluence with Dry Kuy Creek in model layer 2, the drains are present on the banks of the drainage channel and the conductance is based on a 1 foot thick sediment layer (*M*) with a vertical hydraulic conductivity of 2.75 feet/day (*K*) [based on Sand 1 testing (Subsection 2.4.12, Table 2.4.12-14)]. The drain width is the saturated thickness of the drain cell, which is defined by Visual MODFLOW as $\$\Delta Z$, the conductance per unit length (*L*) would be:

$$C/L = 2 \times \frac{2.75 \times \$\Delta Z}{1}$$

The conductance per unit length values are doubled because the drains would be present on both sides of the channel.

**River**

Where river boundaries are overlain by model layers, a hydraulic conductivity of 103 feet/day was assigned to the overlying model cells to allow vertical communication with the river boundary. The hydrogeologic properties (storage and porosity) of these overlying model cells were not changed as these cells are not involved in the particle tracking pathways from the site.

Victoria Barge Canal – A river boundary was assigned on the east side of the model grid to represent the barge canal. A channel bottom of approximately -12 feet and a stage of 0 feet were assigned to represent this sea level canal (Reference 2.4.12-C-14). The boundary was assigned in model layers 6 and 7 as appropriate based on the channel bottom elevation. A vertical hydraulic conductivity of 2.75 feet/day was used with a riverbed thickness of 1 foot. The channel width is 125 feet. A thinner riverbed thickness was assumed for this feature because it is a navigable water body and is regularly dredged.

Coleto Creek – A river boundary was assigned from the western edge of the model to the confluence with the Guadalupe River to represent Coleto Creek. The creek starts in model layer 1 on the west side of the model and ends in layer 5 at the confluence with the Guadalupe River. A linear gradient was used to assign stage and river bottom starting on the west side with a stage of 72 feet and a bottom of 67 feet and ending with a stage of 19 feet and a bottom of 14 feet. The layer assignment for the river boundary was based on the river bottom elevation. As the creek becomes more deeply incised, the boundary condition is assigned to the next lower model layer. The stage elevations were estimated using the mean stage from U.S. Geological Survey gage 8177500 (Reference 2.4.12-C-15). The river conductance was determined using a vertical hydraulic conductivity of 2.75 feet/day and a riverbed thickness of 2 feet. The width of the channel is assumed to be 20 feet.

Guadalupe River – A river boundary was assigned from the north side to the southeast corner of the model domain. A linear gradient was used to assign stage and bottom elevations starting at a stage of 22 feet and a bottom of 10 feet at the north end to a stage of 0 feet and a bottom of -10 feet at the southeast corner. The channel bottom information is derived from channel profiles and the stage is estimated using U.S. Geological Survey stream gage 8177520 data (Reference 2.4.12-C-15). The river boundary is located in model layers 6 and 7 based on the elevation of the channel bottom. A vertical hydraulic conductivity of 2.75 feet/day was used with a riverbed thickness of 2 feet. The width of the channel is 90 feet based on the aforementioned channel profiles.

San Antonio River – A river boundary was assigned from the west side of the model to the southeast side of the model to represent the San Antonio River. The river was represented by two reaches: (a) for the first reach, a linear gradient was used to assign stage and bottom elevations starting at a

stage of 65 feet and a bottom of 40 feet on the west edge of the model domain to a stage of 20 feet and a bottom of 10 feet at U.S. Geological Survey gage 8188570 (Reference 2.4.12-C-15) near U.S. Highway 77, and (b) the second reach, a linear gradient was used to assign stage at bottom elevations starting at a stage of 20 feet and a bottom of 10 feet at U.S. Geological Survey gage 8188570 to a stage of 1 foot and a bottom of -10 feet at the confluence with the Guadalupe River. The San Antonio River starts in model layer 4 on the west side of the model and then is placed in model layer 5 as the channel becomes more deeply incised toward the east. A vertical hydraulic conductivity of 2.75 feet/day was used with a riverbed thickness of 2 feet. The width of the channel is estimated to be 70 feet.

Black Bayou – A river boundary was assigned along Black Bayou in model layers 4 or 5. This boundary corresponds to the eastern limit of the Upper Shallow aquifer in the site area. The stage ranged from 27 feet at the north end to 10 feet at the south end at Linn Lake. The river bottom varied between 26 feet in the north to 7 feet at Linn Lake. A vertical hydraulic conductivity of 2.75 feet/day was used with a riverbed thickness of 2 feet. The width of the Black Bayou channel was assumed to be 20 feet.

**Constant Head**

Linn Lake – A constant head boundary was used to represent the lake. A constant head of 10 feet was assigned in layers 4 or 5. The model cells overlying the constant head cells were assigned a hydraulic conductivity of 103 feet/day to allow communication with the underlying constant head cells. The hydrogeologic properties (storage and porosity) of these overlying model cells were not changed as these cells are not involved in the particle tracking pathways from the site.

### 2.4.12-C-5 Model Calibration

Model calibration involved adjustment of uncertain input parameters to obtain the best match between observed and simulated groundwater levels and the lowest water balance error. The input parameters with the most uncertainty are the recharge rate, because this value is based on regional observations rather than site-specific measurements and hydraulic conductivity. The model was calibrated by systematically varying these parameters over a plausible range to determine the values that yielded the best model fit to the observed potentiometric head data.

#### 2.4.12-C-5.1 Calibration Criteria

The model was considered calibrated when the following criteria were met:

- Residual mean < 2 feet
- Absolute residual mean < 5 feet

- Root mean squared residual < 5 feet
- Normalized root mean squared residual < 10 percent
- Correlation coefficient > 0.8
- Mass balance discrepancy < 1 percent

The residual mean is a measure of the average residual head value defined by the equation:

$$\bar{R} = \frac{1}{n}\sum_{i=1}^{n} R_i$$

(Reference 2.4.12-C-1)

Where,

$n$ = number of observations

$R$ = residual (simulated head $X_{sim}$ – observed head $X_{obs}$)

The absolute residual mean is a measure of the average absolute residual value defined by the equation:

$$\left|\bar{R}\right| = \frac{1}{n}\sum_{i=1}^{n} |R_i|$$

(Reference 2.4.12-C-1)

Where variables are as defined previously.

The root mean squared residual (*RMS*) is defined by:

$$RMS = \sqrt{\frac{1}{n}\sum_{i=1}^{n} R_i^2}$$

(Reference 2.4.12-C-1)

Where variables are as defined previously.

The normalized root mean squared (*NRMS*) residual in the RMS divided by the maximum difference in the observed head values and is determined from:

$$NRMS = \frac{RMS}{(X_{obs})_{\max} - (X_{obs})_{\min}}$$

(Reference 2.4.12-C-1)

Where variables are as defined previously.

The correlation coefficient ($C$) is calculated as the covariance ($COV$) between the simulated head ($X_{sim}$) and the observed head ($X_{obs}$) divided by the product of their standard deviations using the following formulae:

$$C = \frac{COV(X_{sim}, X_{obs})}{\sigma_{sim} \bullet \sigma_{obs}}$$ (Reference 2.4.12-C-1)

$$COV = \frac{1}{n}\sum_{i=1}^{n}(X_i - m_{sim})(X_i - m_{obs})$$ (Reference 2.4.12-C-1)

Where $m_{sim}$ and $m_{obs}$ are the mean values of simulated and observed heads and $\sigma_{sim}$ and $\sigma_{obs}$ are the standard deviations calculated from:

$$\sigma_{sim} = \sqrt{\frac{1}{n}\sum_{i=1}^{n}(X_{sim} - m_{sim})^2}$$ (Reference 2.4.12-C-1)

$$\sigma_{obs} = \sqrt{\frac{1}{n}\sum_{i=1}^{n}(X_{obs} - m_{obs})^2}$$ (Reference 2.4.12-C-1)

The mass balance discrepancy is calculated by MODFLOW 2000 and represents the percent difference between water flow into the model and water flow out of the model.

The simulated and observed heads are typically plotted on a scatter graph, with the X-axis of the graph representing measured values and the Y-axis representing simulated values. A 45° line passing through graph origin (X = Y) represents perfect agreement between observed and simulated values. In addition to the quantitative criteria described above, Visual MODFLOW also includes two qualitative evaluation features. The program calculates the 95 percent confidence interval of the data set and plots this range on the scatter graph. The goal is to have this range bracket the 45° line (X = Y) on the graph. The program also calculates and displays the 95 percent interval of the data, where 95 percent of the total data points are expected to occur. The goal is to bracket the X = Y line and to minimize the width of this range.

### 2.4.12-C-5.2 Summary of Calibrated Model Results

The model calibration process was accomplished in two stages. The first stage involved adjusting the recharge and hydraulic conductivity to obtain the best match between simulated and observed heads. Two recharge zones were established in the model. One zone represented the more permeable surface materials, that is, where sand units outcrop at the surface and the other zone represented the less permeable surface materials. Figure 2.4.12-C-4 presents the location of these

zones, with the blue shaded area representing the more permeable area (Zone 2) and the non-shaded area (Zone 1) representing the less permeable surface materials. After adjustment of these recharge zones, it was found that a recharge rate of 0.4 inch/year for the permeable zone and 0 inch/year for the less permeable zone produced the closest match to observed heads. The less permeable zone is lower than the regional range of recharge, however the regional recharge represents an average over a large area, whereas the VCS model is representative of a much smaller area. The potentiometric surface shown in Figure 2.4.12-C-1 indicates that the Deep aquifer may be influenced by the Guadalupe River and Victoria Barge Canal on the eastern side of the model domain. Initially the modeled heads did not reflect this influence. Review of the stratigraphic model within the Guadalupe River Valley suggests that the clay layers (model layers 7 and 9) have been eroded and replaced with more permeable valley fill deposits. Using the hydraulic conductivity of the underlying sand, the areas of layers 7 and 9 were revised from the original conceptual model within the Guadalupe River Valley, from south of the confluence with Coleto Creek to the southern edge of the model. This allowed the Deep aquifer to be hydraulically connected with the overlying river boundaries in layer 6 (Lower Shallow aquifer). This first stage of calibration produced very good agreement between simulated and observed heads in layers 6, 8, and 10 (or the Lower Shallow and Deep aquifers), however layer 4 heads (Upper Shallow aquifer) did not meet the calibration criteria.

The second stage of calibration focused on layer 4 using an automated calibration program called PEST (Parameter ESTimation) (Reference 2.4.12-C-16). This program is part of the Visual MODFLOW program package. The PEST program adjusts model parameters until the fit between model output (head) and field observations is optimized. PEST utilizes the weighted sum of squared differences between model-generated head values and those actually measured in the field. This sum of weighted, squared, model-to-measurement discrepancies is referred to as the "objective function." The program uses the Gauss-Marquardt-Levenberg algorithm to perform the parameter estimation process. For the VCS groundwater model, the program was constrained to vary the horizontal hydraulic conductivity values for the Upper Shallow aquifer sand in layer 4, which is hydraulic conductivity zone 5 in the model and the vertical hydraulic conductivity of model layer 1, which is hydraulic conductivity zone 7. The initial estimate for hydraulic conductivity was $K_x$,$K_y$ = 60 feet/day in model layer 4 and $K_z$ = 0.068 feet/day in model layer 1. The results suggest that a $K_x$ of 68 feet/day in model layer 4 and $K_z$ of 0.06 feet/day in model layer 1 would improve the model calibration for model layer 4 (Note that layer 1 is dry over virtually all of the model domain. The PEST-estimated K value for the layer 1 clay is therefore uncertain.) Because model layers 2 and 4 are similar materials, the $K_x$ and $K_z$ values used for model layer 4 are also used for model layer 2. These hydraulic conductivity values were used in the model to finalize the calibration. This stage of the calibration process was performed in lieu of a calibration sensitivity analysis.

Figure 2.4.12-C-5 presents the head scatter graph and calibration statistics for the model. Figure 2.4.12-C-6 presents the mass balance for the model. Table 2.4.12-C-7 presents the

measured and simulated heads for the calibration targets. The total mass discrepancy for the calibrated model is 0.04 percent. Based on the calibration statistics and mass balance discrepancy, the model meets the calibration criteria. Model layer 4 exhibits a systematic trend in residuals suggesting that factors other than hydraulic conductivity and recharge are influencing the head distribution in this layer. Figures 2.4.12-C-7 through 2.4.12-C-10 show the simulated potentiometric surface maps for the hydrogeologic units at the site based on current conditions. It should be noted that the jagged or closely spaced contours present on several of the maps represent areas within the layer where a hydraulic conductivity change is occurring, typically a change from sand to clay. Also, model layers 1, 2, and 3 are mostly unsaturated under pre-construction conditions. Figures 2.4.12-C-11 through 2.4.12-C-14 present the calibration residuals for model layers 4 (Upper Shallow aquifer), 6 (Lower Shallow aquifer), 8 (Deep aquifer), and 10 (Deep aquifer).

The Victoria Barge Canal is the primary groundwater sink in the Guadalupe River Valley as indicated by the flow budget presented in Table 2.4.12-C-8.

### 2.4.12-C-6 Predictive Simulations

The predictive simulations performed with the calibrated groundwater flow model include estimation of cooling basin seepage, the amount of water removed during power block area dewatering, and simulation of a post-construction accidental release of radioactive liquid effluent. The following adjustments were made to the pre-construction model for the post-construction conditions:

Surface elevations within the power block area were set to between elevation 90 and 95 feet, and within the cooling basin the surface elevations were set to elevation 69 feet. Areas within the cooling basin where layer 1 was 1 foot in thickness (surficial clay absent as a result of excavation or erosion) were assigned the hydraulic conductivity of the underlying sand.

Permeable backfill and inactive model cells were added to the power block area to represent backfill around buildings and the building foundations.

The ET value of 57.02 inches/year was applied throughout the model domain, with the exception of the cooling basin and power block area building foundations (Figure 2.4.12-C-15).

The layer type for layers 4 through 11 was changed from type 3 to type 0, because these layers are considered to be saturated in post-construction conditions.

The Solver BCLOSE was reduced to between 0.04 and 0.009.

The rewetting settings included a wetting threshold of 0.3.

### 2.4.12-C-6.1 Cooling Basin Seepage

Cooling basin seepage was simulated using the river boundary condition to represent the cooling basin. The river stage for the boundary was set at 90.5 feet with the riverbed bottom at 69 feet. The riverbed conductance is based on a 2 feet thick sediment layer with a $K_v$ = 34 feet/day and a channel width of 500 feet or 250 feet (entire model cell). Figure 2.4.12-C-16 presents a plan view of the boundary conditions in model layer 1.

In addition to the cooling basin, the post-construction power block area conditions were also simulated. Postulated buildings similar to a generic ABWR technology were used to represent buildings within the power block area and were represented by inactive model cells, which were surrounded by cells with permeable backfill. A power block area recharge rate of 0.8 inch/year was assigned to cells not occupied by buildings and a recharge rate of 0 inch/year was assigned within the cooling basin. Figure 2.4.12-C-17 presents the recharge distribution at the cooling basin and power block area. The power block area backfill is assumed to be approximately five times more permeable than the natural sand units; however, mitigating surface features such as finish grading to assure overland flow rather than ponding, storm drains to conduct surface drainage, and vegetation control are assumed to reduce the amount of infiltration through the backfill. The recharge rate for the backfill exceeds the range for the GAM, however, the GAM only represents natural materials.

Cooling basin seepage was evaluated by looking at the flow budget in subareas of the model domain. Visual MODFLOW uses the program ZONEBUDGET to extract the subarea flow budget from the overall model flow budget. The program requires the user to define the subareas or zones within the model for which the flow budget is desired. The following zones were used in the VCS post-construction model:

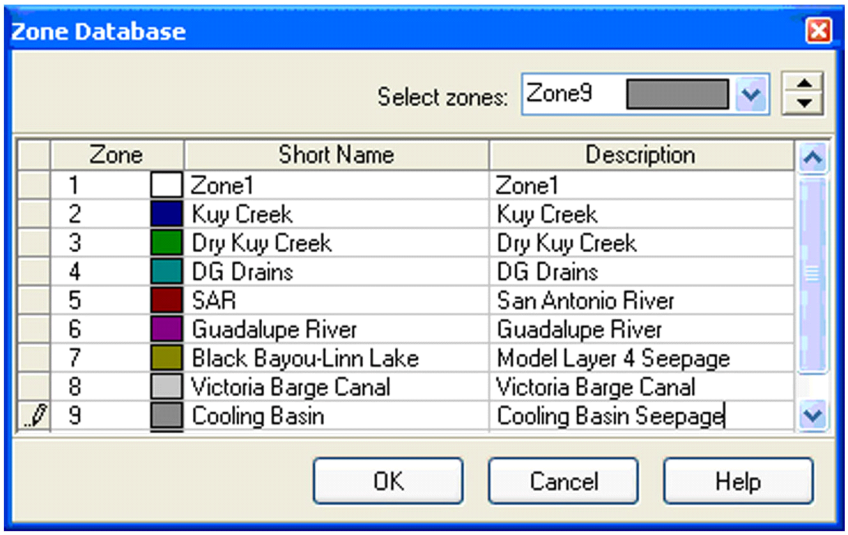

Zone 1 is a default of the program and represents the area of the model not included in other zones. Zone 4 represents the downgradient drains (or seeps) in the Guadalupe River Valley to the north and east of the VCS site. The remaining zone descriptions are self-explanatory.

Figures 2.4.12-C-18 through 2.4.12-C-25 present the pre- and post-construction flow rates for the simulations. It should be noted that there is no pre-construction flow occurring from the cooling basin. These flow rates were converted to gallons per minute (gpm) from $feet^3$/day and are summarized in Table 2.4.12-C-8. The simulation results indicate an estimated 3930 gpm seepage rate from the cooling basin. Kuy Creek, Dry Kuy Creek, and the downgradient seeps show a 220 to 460 gpm increase in base flow (contribution from groundwater). The groundwater contribution to base flow in the Victoria Barge Canal increases by approximately 280 gpm and to the San Antonio River increases by approximately 170 gpm. The Guadalupe River and Black Bayou/Linn Lake flows remain essentially unchanged from the pre- to post-construction conditions.Another impact of cooling basin seepage would be to raise groundwater levels beneath the power block area. Figure 2.4.12-C-26 presents a simulated potentiometric surface map in model layer 2 (geotechnical Sand 1) in the power block area. The map indicates that groundwater levels are predicted to rise after filling the cooling basin. However, the permeable backfill around the power block area buildings provides a pathway for vertical flow to bypass the underlying clay layers and enter the more permeable sands of the Lower Shallow aquifer. The maximum predicted groundwater elevation in the power block area is approximately elevation 85. Figure 2.4.12-C-27 presents a cross-section through the power block area showing groundwater elevations. Figure 2.4.12-C-28 presents the simulated potentiometric surface surrounding the cooling basin in layer 2.

Figure 2.4.12-C-28 indicates an anomalous condition on the Guadalupe River Valley side of the cooling basin. In this area, cells in layers 2 and 4 (geotechnical Sand 1 and Upper Shallow aquifer) are saturated, with a cell in layer 3 (clay) designated as dry. The heads in layers 2 and 4 are rapidly dissipated by boundary conditions (drains in layer 2 and constant heads in layer 4) in the Guadalupe River Valley. This results in insufficient head differential to produce horizontal or vertical flow into layer 3, and hence the layer is dry. Because groundwater flow is occurring primarily in the sands in layers 2 and 4, the presence of these dry cells in the clay (layer 3) should not represent a significant source of error in either flow or head computation.

A sensitivity analysis was performed on uncertain parameters associated with cooling basin seepage. The two primary uncertainties are the conductance of the cooling basin river boundary and the vertical hydraulic conductivity of the natural material underlying the cooling basin.

As discussed previously, the conductance is the product of the surface area and the hydraulic conductivity of the sediment layer divided by the thickness of the sediment (riverbed) layer. The surface area is fixed by the design of the basin, thus the uncertainties are the hydraulic conductivity and the thickness of the sediment or riverbed layer. Because the source of sediment for the cooling

basin is limited to internal sources within the cooling basin and chemical precipitates from the cooling water and a thicker sediment layer would interfere with the proper operation of the cooling basin, a sediment thickness of 2 feet would likely be an upper bound condition. The vertical hydraulic conductivity of the sediment was assumed to be 34 feet/day for the base case, which represents a relatively clean sand. A more likely sediment composition would be that of a silty sand, with a hydraulic conductivity approximately an order of magnitude lower (3.4 feet/day). The first sensitivity case uses this lower hydraulic conductivity to estimate seepage from the cooling basin.

A second sensitivity case involves uncertainty regarding the hydraulic conductivity of the clay in model layer 1. Exposure to repeated wetting and drying cycles could result in a higher hydraulic conductivity of the surficial materials. An order of magnitude increase in vertical hydraulic conductivity (0.6 feet/day) of the clay in layer 1 is assumed for the second sensitivity case.

Table 2.4.12-C-9 presents the results of the sensitivity analysis by comparing the base case seepage rate described above with two sensitivity cases. Figure 2.4.12-C-29 presents the seepage rates for the two sensitivity cases. Sensitivity case 1 appears to be sensitive to a change in the vertical hydraulic conductivity of sediment on the bottom of the cooling basin. An order-of-magnitude reduction in the vertical hydraulic conductivity of the sediment results in an approximately 14.5 percent reduction in the seepage rate from the cooling basin. Sensitivity case 2 appears to be insensitive to a change in the vertical hydraulic conductivity of the surficial clay layer. An order-of-magnitude increase in the vertical hydraulic conductivity of the clay results in only an approximately 2 percent increase in seepage from the cooling basin. The value selected for the hydraulic conductivity of the layer 1 clay in the base case represents the maximum value from the Guelph Permeameter testing and therefore would provide a reasonable estimate for the hydraulic conductivity in the clay.

### 2.4.12-C-6.2 Power Block Area Construction Dewatering Effects

Construction dewatering will be required when constructing the plant because the excavations for the deeper building foundations extend to elevation -15 feet, which is in the Lower Shallow aquifer (model layer 6). The Lower Shallow aquifer is assumed to be dewatered to the approximate bottom of the aquifer at elevation -20 feet. Two dewatering scenarios were considered:

1. Pre-construction groundwater conditions (cooling basin empty) with dewatering the entire power block area.

2. Post-construction groundwater conditions (cooling basin full) with dewatering the entire power block area.

These two scenarios were evaluated because the scheduling of the construction activities is still in the planning stage and these scenarios represent the two extreme conditions. These scenarios would represent the upper and lower bound of dewatering rates for the site. Both scenarios were

simulated by assigning constant head cells in model layers 4 and 6 to represent the dewatering pumping. For the cooling basin full scenario constant head cells were also assigned to model layer 2. Model layer 2 is unsaturated under pre-construction conditions. The head in each constant head cell was set at 1 foot above the bottom of the cell. The interior of the excavation was assigned as inactive cells. Model layers 1, 3, and 5 were treated as no flow boundaries since the flow is primarily vertical within these clay layers.

Table 2.4.12-C-10 presents the results of the simulations. Dewatering pumping (flow) rates ranged from approximately 990 to 1840 gpm. Figures 2.4.12-C-30 through 2.4.12-C-33 present the simulated potentiometric surfaces and cross-sections in the power block area for the dewatering scenarios. The cooling basin full dewatering scenario resulted in further extension of the dry cells in the clay of layer 3 as discussed in Subsection 2.4.12-C-6.1.

### 2.4.12-C-6.3 Accident Release Pathway

The groundwater flow system downgradient of the power block area was evaluated to identify potential exposure points from an accidental release of radionuclides from postulated radwaste facilities. The release is postulated to occur below the basement of a radwaste building in the backfill present in model layer 4 (Upper Shallow aquifer). The release was simulated by placing six particles in the power block area backfill. The movement of these particles was calculated using MODPATH, which is a companion program to MODFLOW that uses its output to perform the particle tracking. Four particle release scenarios are considered:

1. No pumping.
2. With a hypothetical domestic well pumping on the north site boundary (approximately 4500 feet from the release).
3. With a hypothetical domestic well pumping on the west site boundary (approximately 3800 feet from the release).
4. With a hypothetical domestic well pumping on the east site boundary (approximately 11,000 feet from the release).

The hypothetical domestic wells are screened to fully penetrate model layer 6 (Lower Shallow aquifer), which is the uppermost aquifer used for water supply in the site area. Hypothetical water wells located on the site boundary to north and west of the power block area represent the closest locations of a receptor to the accidental release. The well located on the east property boundary represents the most likely receptor based on simulated post-construction groundwater conditions. For the northern well, the screened interval elevation was from -4 to -20 feet, for the western well, the screened interval elevation was from -4 to -31 feet, and for the eastern well, the screened interval

elevation was from 8 to -31 feet. The wells were pumped at 50 gpm, which is considered the maximum practical pumping rate for the Lower Shallow aquifer based on site observations.

Table 2.4.12-C-11 presents a summary of the travel times from the release point to the exposure point at the property boundary as derived from the particle tracking. It should be noted that the MODFLOW simulation is a steady-state solution and is not time-dependent. The MODPATH program uses the velocity components ($V_x$, $V_y$, and $V_z$) to compute the travel time of a particle through each cell. The Visual MODFLOW post-processor displays this travel time at user specified time intervals along each particle track pathway. For all simulations, a travel time interval of 1000 days was specified. Exposure is assumed to occur when a particle reaches the property boundary for the VCS site. The shortest travel time for a particle to reach the property boundary for each scenario is used. The results of the particle tracking indicate a travel time of approximately 41,000 days.

Figure 2.4.12-C-34 presents the particle track pathways for scenario 1. Figure 2.4.12-C-35 shows a cross-section through model row 95 with the particle track pathways. All pathways are projected onto the section. The cross-section indicates that when the particles are released into the fill they migrate down through the fill into model layer 6 (Lower Shallow aquifer) and then travel laterally toward the east-southeast. The particles eventually discharge into Linn Lake, the Guadalupe River, or into the Victoria Barge Canal.

Figures 2.4.12-C-36 and 2.4.12-C-37 present particle tracks for the northern and western pumping scenarios. Neither scenario results in capture of particles by the pumping wells. The primary influence of the offsite pumping is to locally divert the particle tracks toward the north prior to the particle continuing to the eastern site boundary. Figure 2.4.12-C-38 presents the particle tracks for the eastern pumping scenario. For this scenario, the pumping well causes a small deviation in the particle track, but does not capture the particles.

### 2.4.12-C-7 Results

A three-dimensional, eleven-layer groundwater flow model was developed and calibrated to evaluate groundwater level and flow changes associated with the operation of a cooling basin at the VCS site, with dewatering of site excavations, and to assess the impacts of post-construction conditions on the accidental release and transport of radionuclides. This included a reinterpreted conceptual model of the stratigraphy of the model area and incorporation of additional onsite and offsite data that was not available during the previous model development.

Specific findings of the modeling effort include:

- The groundwater levels in the power block area are predicted to be about elevation 85 feet or about 10 feet below the final plant grade of elevation 95 feet.

- The filling of the cooling basin to elevation 90.5 feet is predicted to raise groundwater levels beneath the site to a point where the currently unsaturated sand layer referred to as the Sand 1 geotechnical unit becomes saturated.

- Seepage from the cooling basin is predicted to increase groundwater contributions (base flow) to Kuy and Dry Kuy Creeks and seeps to the north and east of the VCS site. Seepage from the cooling basin is estimated to be approximately 3930 gpm.

- Seepage from the cooling basin is also predicted to alter the groundwater flow directions in the site area, particularly in the power block area.

- Construction dewatering scenarios were simulated with the cooling basin empty and full with an estimated range of pumping rates between 990 (empty) and 1840 gpm (full).

### 2.4.12-C-8 References

Particle tracking suggests that the closest receptor for an accidental release at the power block area would be the eastern property boundary for the VCS site. Pumping of hypothetical domestic wells on the western, eastern, or northern property boundaries did not result in the capture of or significant changes in the flow path of any released particles. The shortest travel time to the property boundary was approximately 41,000 days (110 years) to the eastern site boundary.

2.4.12-C-1 Schlumberger Water Services, *Visual MODFLOW v. 4.3 User's Manual*, Waterloo, Ontario, Canada, 2008.

2.4.12-C-2 Harbaugh, A.W., Banta, E.R., Hill, M.C., and McDonald, M.G., *MODFLOW-2000 The U.S. Geological Survey Modular Ground-Water Model – User Guide to Modularization Concepts and the Ground-Water Flow Process*, U.S. Geological Survey Open-File Report 00-92, Reston, Virginia, 2000.

2.4.12-C-3 Pollock, D.W., *User's Guide for MODPATH/MODPATH-PLOT, version 3: A Particle Tracking Post-Processing Package for MODFLOW, the U.S. Geological Survey Finite-Difference Ground-Water Flow Model*, U.S. Geological Survey Open-File Report 94-464, Reston Virginia, 1994.

2.4.12-C-4 Anderson, M.P. and Woessner, W.W., *Applied Groundwater Modeling Simulation of Flow and Advective Transport*, Academic Press, Inc., San Diego, CA, 1992.

2.4.12-C-5 Chowdhury, A.H. and Turco, M.J., "Geology of the Gulf Coast Aquifer, Texas." in *Aquifers of the Gulf Coast of Texas*, R.E. Mace, S.C. Davidson, E.S. Angle, and W.F. Mullican III eds., Texas Water Development Board Report 365, Austin, TX, 2006.

2.4.12-C-6 National Geodetic Survey, VERTCON North American Vertical Datum Conversion Utility, 2008. Available on line at http://www.ngs.noaa.gov/TOOLS/Vertcon/vertcon.html, accessed June 21, 2008.

2.4.12-C-7 Texas Water Development Board [TWDB], *Water Information Integration & Dissemination (WIID) Groundwater Database*. 2009. Available at http://wiid.twdb.state.tx.us/, accessed September 16 and 18 and October 30, 2009.

2.4.12-C-8 Chowdhury, A.H., Wade, S., Mace, R.E., and Ridgeway, C., *Groundwater Availability Model of the Central Gulf Coast Aquifer System: Numerical Simulations through 1999*, Groundwater Availability Modeling Section, Texas Water Development Board, Austin, TX, 2004.

2.4.12-C-9 Walton, W.C., *Practical Aspects of Groundwater Modeling*, National Water Well Association, Dublin, Ohio, 1984.

2.4.12-C-10 Texas A & M University System, Texas ET Network, administered by the Texas Water Resources Institute of the Texas A & M University System and the Cooperative State Research, Education, and Extension Service of the U.S. Department of Agriculture, 2009. Available at http://texaset.tamu.edu/, accessed December 5, 2009.

2.4.12-C-11 U.S. Geological Survey, *National Elevation Dataset*, 1999. Available at http://gisdata.usgs.net/ned/, accessed October 26, 2009.

2.4.12-C-12 Stüben, K and Clees Tanja, *User's Manual SAMG Release 22c*, Fraunhofer Institute Algorithms and Scientific Computing, St. Augustin, Germany, document version 22c-1.1, 2005.

2.4.12-C-13 Schlumberger Water Services, *Waterloo Hydrogeologic, Inc. presents the Visual MODFLOW Non Convergence Tip Sheet*, 2010. Available at http://www.waterloohydrogeologic.com/support_pdfs/archived-tips-tricks/Non_Convergence_Tips.pdf, accessed January 23, 2010, Waterloo, Ontario, Canada.

2.4.12-C-14 Victoria Economic Development Corporation, *Victoria Barge Canal*, 2006. Available online at http://www.victoriaedc.com/content/view/46/91/, accessed November 11, 2009.

2.4.12-C-15 U.S. Geological Survey, *USGS Surface-Water Daily Statistics for Texas*, 2009. Available online at http://waterdata.usgs.gov/tx/nwis/dvstat?referred_module =sw&county_cd=48469&site_tp_cd=OC&site_tp_cd=OC-CO&site_tp_cd=ES& site_tp_cd=LK&site_tp_cd=ST&site_tp_cd=ST-CA&site_tp_cd=ST-DCH& site_tp_cd=ST-TS&format=station_list&sort_key=site_no&group_key= NONE&list_of_search_criteria=county_cd%2Csite_tp_cd%2Crealtime_parameter_s election, accessed September 27, 2009.

2.4.12-C-16 Watermark Numerical Computing and Waterloo Hydrogeologic Inc., *User's Manual for WinPEST*, Waterloo Hydrogeologic Inc., Waterloo, Ontario, Canada, 1999.

2.4.12-C-17 Cleveland, Theodore G., Bravo, Rolando, and Rogers, Jerry R., Storage Coefficients and Vertical Hydraulic Conductivities in Aquitards Using Extensometer and Hydrograph Data, Ground Water, Vol. 30, No. 5, pp 701-708, 1992.

2.4.12-C-18 Fetter, C.W., Applied Hydrogeology, 3rd Edition, 1994.

**Table 2.4.12-C-1 (Sheet 1 of 2)**
**VCS Site Average Groundwater Level Elevations**

| Well | Easting (ft) | Northing (ft) | Unit[a] | Mean Groundwater Elevation (ft NAVD 88) | Screen Midpoint Elevation (ft NAVD 88) |
|---|---|---|---|---|---|
| OW-01L | 2606687 | 13404252 | Lower | 30.00 | -32.8 |
| OW-01U | 2606667 | 13404254 | Upper | 30.73 | 17.2 |
| OW-02L | 2607869 | 13411521 | Lower | 24.31 | -27.9 |
| OW-02U | 2607862 | 13411502 | Upper | 24.55 | 17.3 |
| OW-03L | 2609287 | 13414919 | Lower | 19.03 | -16.8 |
| OW-3U[b] | 2609295 | 13414934 | Upper | Dry | 27.6 |
| OW-04L | 2607440 | 13414269 | Lower | 22.62 | -25.9 |
| OW-04U | 2607429 | 13414281 | Upper | 23.59 | 25[c] |
| OW-05L | 2605813 | 13414774 | Deep | 25.61 | -46.7 |
| OW-05U | 2605832 | 13414770 | Upper | 26.07 | 27.1 |
| OW-06L | 2604965 | 13415890 | Lower | 26.19 | -10.5 |
| OW-06U | 2604967 | 13415876 | Upper | 26.35 | 21.5 |
| OW-07L | 2606531 | 13418421 | Deep | 19.62 | -40.5 |
| OW-07U | 2606542 | 13418421 | Upper | 19.91 | 19.3 |
| OW-08L | 2598942 | 13415819 | Deep | 32.54 | -49.4 |
| OW-08U | 2598935 | 13415801 | Lower | 36.02 | -12.6 |
| OW-09L | 2604894 | 13414937 | Deep | 27.17 | -32[c] |
| OW-09U | 2604895 | 13414956 | Upper | 26.93 | 22.9 |
| OW-10L | 2604761 | 13418486 | Deep | 23.48 | -53.9 |
| OW-10U | 2604768 | 13418474 | Upper | 22.27 | 25.1 |
| OW-2150L | 2599585 | 13412553 | Deep | 33.22 | -56[c] |
| OW-2150U | 2599583 | 13412568 | Upper | 44.85 | 20.9 |
| OW-2169L | 2599930 | 13412357 | Lower | 35.45 | -15 |
| OW-2169U | 2599946 | 13412344 | Upper | 41.92 | 20.1 |
| OW-2181L | 2600072 | 13412138 | Lower | 35.64 | -15.1 |
| OW-2181U | 2600053 | 13412147 | Upper | 41.62 | 35 |
| OW-2185L | 2600816 | 13412314 | Lower | 34.12 | -15.2 |
| OW-2185U | 2600801 | 13412328 | Upper | 38.30 | 9.9 |
| OW-2253L[d] | 2600474 | 13413592 | Deep | 31.88 | -58.8 |
| OW-2253U[d] | 2600495 | 13413585 | Upper | 45.40 | 21.2 |
| OW-2269L | 2600574 | 13413123 | Deep | 32.03 | -54.1 |
| OW-2269U | 2600589 | 13413110 | Lower | 34.03 | -12[c] |
| OW-2284L | 2600939 | 13413064 | Lower | 33.63 | -24 |
| OW-2284U | 2600957 | 13413055 | Upper | 42.75 | 11 |

**Table 2.4.12-C-1 (Sheet 2 of 2)**
**VCS Site Average Groundwater Level Elevations**

| Well | Easting (ft) | Northing (ft) | Unit[a] | Mean Groundwater Elevation (ft NAVD 88) | Screen Midpoint Elevation (ft NAVD 88) |
|---|---|---|---|---|---|
| OW-2301L | 2596268 | 13414430 | Deep | 36.75 | -53.1 |
| OW-2301U | 2596288 | 13414430 | Upper | 49.25 | 26.8 |
| OW-2302L | 2598389 | 13407382 | Deep | 35.56 | -60[c] |
| OW-2302U | 2598388 | 13407362 | Lower | 37.30 | -9.5 |
| OW-2304L | 2608678 | 13396528 | Lower | 26.19 | -21.1 |
| OW-2304U | 2608679 | 13396542 | Upper | 34.12 | 23.8 |
| OW-2307L | 2603152 | 13420879 | Lower | 24.57 | -28.1 |
| OW-2307U | 2603164 | 13420897 | Upper | 31.39 | 17.1 |
| OW-2319L | 2603052 | 13403611 | Deep | 32.87 | -75.3 |
| OW-2319U | 2603046 | 13403590 | Lower | 33.95 | -15.7 |
| OW-2320L | 2606834 | 13407581 | Deep | 28.73 | -73.2 |
| OW-2320U | 2606850 | 13407570 | Lower | 27.75 | -33.2 |
| OW-2321L | 2610028 | 13410955 | Deep | 20.23 | -73 |
| OW-2321U | 2610041 | 13410944 | Lower | 20.40 | -33.2 |
| OW-2324L | 2612217 | 13416301 | Deep | 12.28 | -95.1 |
| OW-2324U | 2612203 | 13416317 | Lower | 12.74 | -15.3 |
| OW-2348L | 2621644 | 13409618 | Deep | 11.14 | -87.8 |
| OW-2348U | 2621661 | 13409636 | Lower | 10.91 | -24.4 |
| OW-2352L | 2617519 | 13402468 | Lower | 18.86 | -21.7 |
| OW-2352U | 2617539 | 13402471 | Upper | 18.83 | 13.2 |
| OW-2359L1 | 2605471 | 13417264 | Deep | 22.94 | -88.9 |
| OW-2359U1 | 2605461 | 13417253 | Lower | 22.94 | -12.3 |
| 7923601 | 2561712 | 13437903 | Deep | 68.91 | 4 |
| 7924102 | 2581676 | 13448023 | Deep | 48.90 | 3 |
| 7924702 | 2572205 | 13427869 | Deep | 58.44 | -63.4 |

(a) Unit: Upper = Upper Shallow aquifer; Lower = Lower Shallow aquifer; Deep = Deep aquifer
(b) Not used for model calibration target
(c) Screen midpoint elevation adjusted to place observation well in the appropriate hydrogeologic unit
(d) Groundwater elevation data corrected for revised reference elevation

**Table 2.4.12-C-2 (Sheet 1 of 4)**
**TWDB Groundwater Levels Used to Prepare Regional Potentiometric Surface Map**

| Well | Easting (ft) | Northing (ft) | Type | Date | Unit | Static Level (ft bgs) | Groundwater Elevation (NAVD 88) | Screen Midpoint Elevation (NAVD 88) |
|---|---|---|---|---|---|---|---|---|
| 2975 | 2629306 | 13423478 | Domestic | 10/17/2001 | Deep | 13 | -4 | -118 |
| 2976 | 2630562 | 13422995 | Domestic | 10/18/2001 | Deep | 16 | 8 | -116 |
| 3395 | 2593942 | 13444084 | Domestic | 11/16/2001 | Deep | 63 | 25 | -57 |
| 12527 | 2591656 | 13442329 | Domestic | 9/18/2002 | Lower | 57 | 31 | 1 |
| 13049 | 2635570 | 13437024 | Domestic | 7/25/2001 | Lower | 45 | 19 | -6 |
| 15387 | 2584676 | 13455143 | Domestic | 10/31/2002 | Lower | 44 | 33 | -9 |
| 15388 | 2584676 | 13455143 | Domestic | 12/13/2002 | Deep | 42 | 35 | -41 |
| 20512 | 2557613 | 13420970 | Domestic | 5/16/2003 | Lower | 47 | 67 | -1 |
| 20516 | 2558217 | 13422192 | Domestic | 5/17/2003 | Lower | 43 | 70 | -2 |
| 20754 | 2558534 | 13424722 | Domestic | 5/23/2003 | Lower | 51 | 60 | -4 |
| 20756 | 2556606 | 13422672 | Domestic | 5/24/2003 | Lower | 51 | 63 | -26 |
| 21203 | 2553283 | 13441508 | Domestic | 6/2/2003 | Deep | 45 | 76 | -69 |
| 28288 | 2650367 | 13451230 | Domestic | 8/22/2003 | Lower | 31 | 29 | -37 |
| 28700 | 2614329 | 13397964 | Industrial | 6/6/2003 | Deep | 55 | 9 | -186 |
| 29459 | 2638583 | 13447886 | Domestic | 8/8/2003 | Lower | 40 | 24 | -41 |
| 29661 | 2572086 | 13446352 | Domestic | 9/9/2003 | Lower | 40 | 66 | -39 |
| 30482 | 2587888 | 13443983 | Domestic | 10/17/2003 | Lower | 50 | 40 | 6 |
| 30484 | 2580697 | 13431643 | Stock | 10/21/2003 | Lower | 49 | 46 | -23 |
| 30487 | 2581098 | 13434377 | Stock | 10/23/2003 | Lower | 47 | 48 | 5 |
| 35570 | 2642383 | 13414821 | Rig Supply | 4/7/2004 | Deep | 50 | -24 | -84 |
| 37824 | 2595814 | 13390680 | Domestic | 8/29/2003 | Deep | 47 | 13 | -70 |
| 38317 | 2623846 | 13450352 | Domestic | 3/16/2004 | Lower | 19 | 22 | -28 |
| 39830 | 2620351 | 13441402 | Public Supply | 6/19/2004 | Deep | 13.5 | 22 | -201 |
| 40870 | 2565386 | 13447659 | Domestic | 7/8/2004 | Lower | 48 | 60 | 3 |
| 40876 | 2557985 | 13425622 | Domestic | 7/15/2004 | Lower | 46 | 65 | -9 |
| 41862 | 2630239 | 13456425 | Domestic | 7/26/2004 | Lower | 50 | 23 | -32 |
| 44703 | 2564716 | 13433810 | Domestic | 9/10/2004 | Upper | 48 | 62 | 17 |
| 46887 | 2553498 | 13416259 | Domestic | 9/27/2004 | Lower | 49 | 52 | -36 |
| 46888 | 2566591 | 13455860 | Domestic | 9/29/2004 | Lower | 35 | 58 | -22 |
| 47169 | 2564716 | 13433810 | Domestic | 10/15/2004 | Upper | 48 | 62 | 30 |
| 47194 | 2610571 | 13383050 | Domestic | 10/21/2004 | Deep | 10 | 16 | -109 |
| 47734 | 2586128 | 13448096 | Domestic | 10/27/2004 | Upper | 54 | 41 | 15 |
| 49428 | 2560160 | 13372424 | Domestic | 7/9/2003 | Deep | 23 | 62 | -100 |
| 51472 | 2574592 | 13373866 | Domestic | 2/18/2004 | Deep | 40 | 42 | -223 |
| 52185 | 2592889 | 13400328 | Domestic | 1/13/2004 | Lower | 42 | 36 | -33 |
| 53341 | 2568845 | 13431855 | Domestic | 1/21/2005 | Deep | 55 | 51 | -142 |
| 55969 | 2625500 | 13447452 | Domestic | 2/18/2005 | Lower | 35 | 24 | -7 |

**Table 2.4.12-C-2 (Sheet 2 of 4)**
**TWDB Groundwater Levels Used to Prepare Regional Potentiometric Surface Map**

| Well | Easting (ft) | Northing (ft) | Type | Date | Unit | Static Level (ft bgs) | Groundwater Elevation (NAVD 88) | Screen Midpoint Elevation (NAVD 88) |
|---|---|---|---|---|---|---|---|---|
| 56174 | 2616736 | 13392854 | Stock | 1/27/2005 | Deep | 44 | 18 | -54 |
| 58542 | 2563763 | 13448946 | Domestic | 3/17/2005 | Deep | 41 | 60 | -117 |
| 62190 | 2625774 | 13447053 | Domestic | 12/17/2003 | Lower | 40 | 20 | -32 |
| 62191 | 2625774 | 13447053 | Domestic | 12/29/2003 | Lower | 27 | 33 | -20 |
| 63332 | 2566198 | 13435853 | Domestic | 6/2/2005 | Upper | 42 | 68 | 27 |
| 63333 | 2567877 | 13442244 | Domestic | 6/3/2005 | Upper | 42 | 68 | 40 |
| 66473 | 2552514 | 13445133 | Domestic | 9/3/2005 | Deep | 55 | 61 | -171 |
| 70190 | 2650361 | 13461331 | Rig Supply | 10/26/2005 | Deep | 33 | 32 | -65 |
| 72241 | 2649345 | 13453534 | Domestic | 10/14/2005 | Lower | 30 | 32 | -16 |
| 74199 | 2650274 | 13461228 | Irrigation | 1/2/2006 | Deep | 33 | 32 | -500 |
| 79458 | 2637407 | 13383923 | Rig Supply | 1/29/2006 | Deep | 32 | -23 | -177 |
| 80941 | 2582807 | 13449657 | Rig Supply | 2/28/2006 | Deep | 38 | 34 | -113 |
| 83861 | 2597763 | 13428693 | Domestic | 3/28/2006 | Deep | 57 | -8 | -62 |
| 83923 | 2579059 | 13367979 | Rig Supply | 4/3/2006 | Deep | 50 | 27 | -113 |
| 84813 | 2593692 | 13437716 | Domestic | 5/5/2006 | Lower | 52 | 20 | -28 |
| 87073 | 2550192 | 13445501 | Domestic | 7/7/2006 | Lower | 45 | 76 | -14 |
| 90311 | 2637916 | 13435348 | Domestic | 1/10/2003 | Deep | 47 | 13 | -70 |
| 90980 | 2561827 | 13424976 | Domestic | 6/30/2006 | Deep | 43 | 65 | -52 |
| 91796 | 2556196 | 13443170 | Domestic | 7/5/2006 | Lower | 32 | 87 | -16 |
| 94678 | 2591928 | 13393747 | Domestic | 8/26/2003 | Upper | 47 | 38 | 5 |
| 96505 | 2577972 | 13429376 | Domestic | 8/30/2006 | Deep | 53 | 45 | -82 |
| 96509 | 2577972 | 13429376 | Domestic | 8/30/2006 | Deep | 53 | 45 | -82 |
| 97825 | 2633786 | 13422143 | Domestic | 9/16/2006 | Deep | 55 | 5 | -48 |
| 105177 | 2594099 | 13434692 | Domestic | 2/26/2007 | Lower | 55 | 30 | -20 |
| 109093 | 2646705 | 13456719 | Domestic | 2/17/2007 | Deep | 35 | 29 | -41 |
| 109312 | 2584679 | 13427870 | Stock | 2/24/2007 | Lower | 60 | 33 | -17 |
| 111653 | 2595760 | 13457852 | Irrigation | 4/30/2007 | Deep | 43 | 39 | -108 |
| 114737 | 2567667 | 13394059 | Domestic | 6/15/2007 | Deep | 23 | 52 | -55 |
| 114765 | 2577096 | 13373503 | Rig Supply | 5/31/2007 | Deep | 36 | 42 | -62 |
| 116813 | 2554345 | 13441929 | Domestic | 6/18/2007 | Lower | 45 | 74 | -22 |
| 123730 | 2567559 | 13400825 | Domestic | 9/4/2007 | Lower | 40 | 45 | -6 |
| 123876 | 2579019 | 13375958 | Rig Supply | 9/26/2007 | Deep | 42 | 33 | -60 |
| 125118 | 2577379 | 13449468 | Domestic | 9/30/2007 | Lower | 51 | 47 | -16 |
| 125240 | 2553568 | 13451715 | Domestic | 1/11/2005 | Lower | 34 | 64 | -2 |
| 126101 | 2597208 | 13413936 | Industrial | 10/31/2007 | Deep | 45 | 37 | -78 |
| 126247 | 2589607 | 13399264 | Domestic | 10/21/2007 | Deep | 43 | 42 | -110 |
| 126971 | 2561423 | 13416687 | Rig Supply | 10/29/2007 | Deep | 53 | 58 | -53 |
| 128362 | 2639296 | 13422948 | Domestic | 11/23/2007 | Deep | 43 | 16 | -254 |
| 129682 | 2593494 | 13396096 | Rig Supply | 11/1/2007 | Deep | 44 | 39 | -57 |

**Table 2.4.12-C-2 (Sheet 3 of 4)**
**TWDB Groundwater Levels Used to Prepare Regional Potentiometric Surface Map**

| Well | Easting (ft) | Northing (ft) | Type | Date | Unit | Static Level (ft bgs) | Groundwater Elevation (NAVD 88) | Screen Midpoint Elevation (NAVD 88) |
|---|---|---|---|---|---|---|---|---|
| 129733 | 2585664 | 13395057 | Rig Supply | 11/13/2007 | Deep | 50 | 38 | -132 |
| 129891 | 2596667 | 13393017 | Rig Supply | 11/29/2007 | Deep | 55 | 30 | -55 |
| 131103 | 2621991 | 13459714 | Domestic | 11/29/2007 | Lower | 24 | 22 | -26 |
| 131109 | 2647137 | 13427938 | Domestic | 11/3/2007 | Deep | 40 | 17 | -114 |
| 133529 | 2595195 | 13390367 | Rig Supply | 12/28/2007 | Deep | 47 | 28 | -95 |
| 134709 | 2594186 | 13386713 | Rig Supply | 2/8/2008 | Deep | 24 | 18 | -83 |
| 134712 | 2578197 | 13382612 | Rig Supply | 2/4/2008 | Deep | 13 | 32 | -70 |
| 136966 | 2571958 | 13371198 | Rig Supply | 2/27/2008 | Lower | 30 | 48 | 0 |
| 137968 | 2572442 | 13446358 | Domestic | 3/28/2008 | Lower | 50 | 55 | -5 |
| 138301 | 2549695 | 13460341 | Domestic | 2/6/2007 | Lower | 38 | 73 | -12 |
| 138492 | 2557861 | 13427843 | Stock | 4/1/2008 | Lower | 34 | 79 | 3 |
| 139366 | 2573143 | 13375156 | Rig Supply | 3/14/2008 | Deep | 25 | 52 | -93 |
| 139380 | 2566733 | 13368690 | Rig Supply | 3/24/2008 | Deep | 29 | 49 | -67 |
| 140059 | 2598215 | 13401730 | Rig Supply | 4/1/2008 | Deep | 38 | 37 | -75 |
| 142684 | 2563200 | 13439543 | Domestic | 10/22/2004 | Lower | 44 | 67 | -4 |
| 142764 | 2578594 | 13374638 | Rig Supply | 4/30/2008 | Lower | 42 | 36 | -32 |
| 143295 | 2566186 | 13419793 | Rig Supply | 5/13/2008 | Deep | 42 | 63 | -68 |
| 143694 | 2580145 | 13449109 | Rig Supply | 6/1/2008 | Deep | 44 | 48 | -156 |
| 146005 | 2636438 | 13438352 | Domestic | 5/15/2008 | Deep | 35 | 27 | -106 |
| 146330 | 2650857 | 13370326 | Domestic | 6/2/2008 | Deep | -2 | 6 | -146 |
| 147246 | 2599419 | 13441448 | Domestic | 7/9/2008 | Lower | 22 | 24 | -34 |
| 148624 | 2642567 | 13429371 | Stock | 2/12/2006 | Deep | 44 | 15 | -85 |
| 148628 | 2633111 | 13369604 | Stock | 2/17/2006 | Deep | 1 | 8 | -57 |
| 148634 | 2572856 | 13431718 | Domestic | 3/9/2006 | Lower | 50 | 55 | -39 |
| 150946 | 2630378 | 13367737 | Industrial | 8/22/2005 | Deep | 2 | 39 | -179 |
| 151183 | 2643671 | 13367974 | Domestic | 7/18/2005 | Deep | 28 | 13 | -119 |
| 152378 | 2550222 | 13443582 | Domestic | 8/6/2005 | Deep | 50 | 71 | -61 |
| 153420 | 2592162 | 13390417 | Rig Supply | 8/8/2008 | Deep | 37 | 35 | -118 |
| 155221 | 2553252 | 13392013 | Stock | 8/14/2008 | Deep | 30 | 68 | -62 |
| 155301 | 2642071 | 13442089 | Industrial | 10/4/2008 | Deep | 37 | 23 | -206 |
| 156209 | 2551353 | 13393701 | Industrial | 6/24/2005 | Deep | 40 | 58 | -72 |
| 157382 | 2590715 | 13375443 | Rig Supply | 9/2/2008 | Deep | 38 | 39 | -53 |
| 157386 | 2580339 | 13382546 | Rig Supply | 9/3/2008 | Deep | 10 | 39 | -81 |
| 161253 | 2593997 | 13419438 | Stock | 10/8/2008 | Deep | 45 | 40 | -67 |
| 161358 | 2609667 | 13368085 | Rig Supply | 10/16/2008 | Deep | 30 | 30 | -70 |
| 161644 | 2623066 | 13449127 | Domestic | 12/5/2008 | Deep | 18 | 24 | -63 |
| 161646 | 2592521 | 13433151 | Stock | 12/8/2008 | Lower | 47 | 38 | -30 |
| 161688 | 2581900 | 13407117 | Rig Supply | 9/17/2008 | Deep | 39 | 46 | -65 |
| 165912 | 2572413 | 13420498 | Rig Supply | 11/6/2008 | Lower | 43 | 57 | -30 |

**Table 2.4.12-C-2 (Sheet 4 of 4)**
**TWDB Groundwater Levels Used to Prepare Regional Potentiometric Surface Map**

| Well | Easting (ft) | Northing (ft) | Type | Date | Unit | Static Level (ft bgs) | Groundwater Elevation (NAVD 88) | Screen Midpoint Elevation (NAVD 88) |
|---|---|---|---|---|---|---|---|---|
| 166025 | 2575389 | 13418324 | Rig Supply | 11/7/2008 | Lower | 44 | 51 | -35 |
| 167501 | 2569737 | 13459546 | Domestic | 2/3/2009 | Deep | 72 | 26 | -62 |
| 169413 | 2572955 | 13381315 | Stock | 2/19/2009 | Deep | 15 | 37 | -128 |
| 169935 | 2560570 | 13431219 | Domestic | 6/20/2005 | Upper | 43 | 71 | 38 |
| 169956 | 2562731 | 13452263 | Domestic | 12/30/2004 | Deep | 40 | 58 | -81 |
| 170172 | 2605749 | 13399130 | Rig Supply | 4/22/2005 | Deep | 50 | 20 | -142 |
| 170186 | 2633755 | 13459012 | Domestic | 8/2/2004 | Lower | 41 | 34 | -25 |
| 170597 | 2586817 | 13449521 | Domestic | 12/2/2004 | Upper | 24 | 40 | 34 |
| 170601 | 2588963 | 13443597 | Domestic | 7/16/2004 | Deep | 50 | 42 | -108 |
| 170670 | 2628169 | 13447600 | Domestic | 1/3/2009 | Lower | 34 | 25 | -23 |
| 170672 | 2581053 | 13437103 | Domestic | 3/10/2009 | Lower | 50 | 45 | -5 |
| 171010 | 2610853 | 13366590 | Domestic | 2/2/2009 | Deep | 35 | 22 | -123 |
| 183355 | 2576314 | 13372177 | Rig Supply | 5/14/2009 | Deep | 36 | 44 | -110 |
| 185268 | 2572167 | 13446858 | Domestic | 5/25/2009 | Lower | 35 | 70 | -5 |
| 187268 | 2563774 | 13408946 | Stock | 7/10/2009 | Deep | 50 | 55 | -63 |
| 187653 | 2561835 | 13441340 | Domestic | 6/30/2009 | Lower | 42 | 68 | -30 |
| 191003 | 2584205 | 13380690 | Rig Supply | 7/27/2009 | Deep | 9 | 36 | -75 |

Unit: Upper = Upper Shallow aquifer; Lower = Lower Shallow aquifer; Deep = Deep aquifer
NAVD 88 = North American Vertical Datum of 1988
ftbgs = feet below ground surface

## Table 2.4.12-C-3
## Harmonic Mean Vertical Hydraulic Conductivity of Layer 11

| Well | Northing | Easting | Elevation (NAVD88) | Total Depth (ftbgs) | Sand 6 | | Clay 7 | | Sand 8 | | Clay 9 | | Sand 10 | | |
|---|---|---|---|---|---|---|---|---|---|---|---|---|---|---|---|
| | | | | | Depth Bottom | Elev. Bottom | Depth Bottom | Thickness | Depth Bottom | Thickness | Depth Bottom | Thickness | Depth Bottom | Thickness | |
| 129733 | 13395057 | 2585664.09 | 88 | 240 | 191.0 | -102.9 | 206 | 15 | | | | | | | |
| 143580 | 13380355 | 2588403.74 | 39 | 275 | 120.0 | -81.1 | 157 | 37 | 171 | 14 | 210 | 39 | 227 | 17 | |
| 143991 | 13386642 | 2636912.87 | 32 | 264 | 155.0 | -122.6 | 180 | 25 | 233 | 53 | 248 | 15 | | | |
| 153420 | 13390417 | 2592161.86 | 72 | 250 | 214.0 | -142.3 | 238 | 24 | | | | | | | |
| 39830 | 13441402 | 2620350.8 | 36 | 260 | 167.0 | -131.3 | 196 | 29 | 207 | 11 | | | | | |
| 68027 | 13419465 | 2630892.05 | 14 | 180 | 140.0 | -125.7 | 155 | 15 | | | | | | | |
| 68823 | 13415933 | 2619545.85 | 14 | 140 | 95.0 | -80.7 | 105 | 10 | | | | | | | |
| B-2301 | 13414430 | 2596278.37 | 80.79 | 300 | 194.0 | -113.2 | 240 | 46 | 265 | 25 | 292 | 27 | | | |
| B-2302 | 13407371 | 2598389.3 | 80 | 315 | 181.0 | -101.0 | 227 | 46 | 273 | 46 | | | | | |
| B-2303 | 13402308 | 2600478.63 | 75.56 | 310 | 192.0 | -116.4 | 234 | 42 | 265 | 31 | | | | | |
| B-2304 | 13396556 | 2608686.75 | 68.12 | 310 | 235.0 | -166.9 | 236 | | 288 | 52 | | | | | |
| B-2305 | 13406653 | 2621646.04 | 65.58 | 305 | 185.2 | -119.6 | 238.8 | 54 | 250 | 11 | | | | | |
| B-2306 | 13411450 | 2615249.64 | 64.68 | 310 | 196.0 | -131.3 | 220 | 24 | 231 | 11 | | | | | |
| B-2307 | 13420888 | 2603157.79 | 76.38 | 310 | 189.0 | -112.6 | 190 | | 238.2 | 48 | 282 | 44 | | | |
| B-11 | 13411479 | 2607866.27 | 74.5 | 310 | 205.0 | -130.5 | 220 | 15 | 240 | 20 | 260 | 20 | 295 | 35 | |
| B-2169 | 13412350 | 2599938.43 | 79.46 | 400 | 213.5 | -134.0 | 253 | 40 | 284 | 31 | 326 | 42 | 334 | 8 | |
| B-2170 | 13412414 | 2599989.73 | 79.72 | 300 | 197.0 | -117.3 | 258.5 | 62 | 288.5 | 30 | | | | | |
| B-2170R | 13412396 | 2599989.34 | 79.17 | 300 | 203.0 | -123.8 | 268.5 | 66 | 288.5 | 20 | | | | | |
| B-2171R | 13412480 | 2600074.23 | 79.97 | 300 | 219.2 | -139.2 | 255 | 36 | 285 | 30 | | | | | |
| B-2173 | 13412225 | 2599944.53 | 79.6 | 300 | 228.5 | -148.9 | 257 | 29 | 287 | 30 | | | | | |
| B-2174A | 13412299 | 2600000.66 | 80.1 | 601 | 212.0 | -131.9 | 243 | 31 | 284.6 | 42 | 321.8 | 37 | 335.5 | 14 | |
| B-2182A | 13412207 | 2600143.8 | 79.5 | 399.8 | 207.5 | -127.8 | 230.5 | 23 | 284.6 | 54 | 348.6 | 64 | 373.2 | 25 | |
| B-2269 | 13413117 | 2600582.5 | 80.45 | 403.3 | 201.7 | -121.3 | 202.7 | | 301.8 | 99 | 322.6 | 21 | | | |
| B-2270 | 13413179 | 2600633.41 | 80.62 | 300 | 218.5 | -137.9 | 219.5 | | 258.5 | 39 | | | | | |
| B-2271 | 13413253 | 2600735.25 | 80.46 | 301.2 | 209.0 | -128.5 | 210 | | 281 | 71 | | | | | |
| B-2273 | 13412991 | 2600585.52 | 80.69 | 399.4 | 217.9 | -137.2 | 218.9 | | 291 | 72 | 334 | 43 | 367.9 | 34 | |
| B-2274A | 13413066 | 2600642.97 | 80.86 | 594.7 | 220.0 | -139.1 | 221 | | 290 | 69 | 327 | 37 | 368.2 | 41 | |
| B-2282A | 13412971 | 2600757.69 | 80.31 | 400 | 218.5 | -138.2 | 219.5 | | 285 | 66 | 331 | 46 | 373 | 42 | Total |
| | | Layer not present | | | | Average Thickness (ft) | | 33 | | 41 | | 36.2 | | 26.9 | 137 |
| | | below bottom of the boring/well | | | | Fraction of thickness ($w$) | | 0.24 | | 0.30 | | 0.26 | | 0.20 | 1.00 |
| | | | | | | $K_v$ (ft/d) [$x$] | | 7.00E-05 | | 34 | | 7.00E-05 | | 34 | |

weighted harmonic mean 0.000138 ft/d

$$wHM = \frac{1}{\frac{w_1}{x_1} + \frac{w_2}{x_2} + \cdots \frac{w_n}{x_n}}$$

## Table 2.4.12-C-4
## Hydraulic Conductivity Values

| Model Layer[a] | Geotechnical Layer | Model Horizontal Hydraulic Conductivity $K_h$ (ft/day) | Source | Model Vertical Hydraulic Conductivity $K_v$ (ft/day) | Source |
|---|---|---|---|---|---|
| 1 | Clay 1 Top | 0.68[b] | Reference 2.4.12-C-9 | 0.068[b] | Table 2.4.12-14 |
| 2 | Sand 1 | 8.2[c] | Reference 2.4.12-C-9 | 2.75[c] | Table 2.4.12-14 |
| 3 | Clay 1 Bottom | $7 \times 10^{-4}$ | Reference 2.4.12-C-9 | $7 \times 10^{-5}$ | Table 2.4.12-13 |
| 4 | Sand 2 | 60[c] | Table 2.4.12-9[d] | 20[c] | Reference 2.4.12-C-9 |
| 5 | Clay 3 | $7 \times 10^{-4}$ | Reference 2.4.12-C-9 | $7 \times 10^{-5}$ | Table 2.4.12-13 |
| 6 | Sand 4 | 103[e] | Table 2.4.12-9[d] | 34 | Reference 2.4.12-C-9 |
| 7 | Clay 5 Top | $7 \times 10^{-4}$ | Reference 2.4.12-C-9 | $7 \times 10^{-5}$ | Table 2.4.12-13 |
| 8 | Sand 5 | 103[e] | Table 2.4.12-9[e] | 34 | Reference 2.4.12-C-9 |
| 9 | Clay 5 Bottom | $7 \times 10^{-4}$ | Reference 2.4.12-C-9 | $7 \times 10^{-5}$ | Table 2.4.12-13 |
| 10 | Sand 6 | 103[e] | Table 2.4.12-9[e] | 34 | Reference 2.4.12-C-9 |
| 11 | Clay 7 and 9<br>Sand 8 and 10 | $1.4 \times 10^{-3}$ | Reference 2.4.12-C-9 | $1.4 \times 10^{-4}$ | Table 2.4.12-C-3 |

(a) Where geotechnical layers are absent in a given model layer, the underlying layer hydraulic conductivity is used.
(b) Adjusted during calibration – model layer 1 $K_v$ = 0.06 feet/day and $K_h$ = 0.6 feet/day
(c) Adjusted during calibration – model layers 2 and 4 $K_h$ = 68 feet/day and Kv = 23 feet/day
(d) Table 2.4.12-9 was revised to include the updated hydraulic conductivity after re-interpretation of the saturated thickness for Upper Shallow and Deep aquifers. The groundwater modeling values for hydraulic conductivity of the sand layers are higher but matched favorably with the hydraulic conductivity values in Reference 2.5.4-2 and meet the model calibration criteria as discussed in Subsection 2.4.12-C-5.
(e) Adjusted during calibration – model layers 6, 8, and 10 to $K_h$ = 103 feet/day and $K_v$ = 34 feet/day

Note:$K_h$ of Sand 2 determined from 48-hour pumping test of TW-2320U in Sand 2. $K_h$ of Sand 4, Sand 5, and Sand 6 determined from 24-hour pumping test of TW-2359L in Sand 5. $K_h$ of Sand 4, Sand 5, and Sand 6 assumed to be equal based on grain size analysis.

**Table 2.4.12-C-5**
**Porosity Values**

| Model Layer | Geotechnical Unit | Mean Total Porosity (%) | Mean Effective Porosity (%) |
|---|---|---|---|
| 1 | Clay 1 Top | 35.8 | 7.2 |
| 2 | Sand 1 | 31.0 | 24.7 |
| 3 | Clay 1 Bottom | 40.5 | 8.1 |
| 4 | Sand 2 | 36.6 | 29.2 |
| 5 | Clay 3 | 41.4 | 8.3 |
| 6 | Sand 4 | 36.5 | 29.2 |
| 7 | Clay 5 Top | 38.1 | 7.8 |
| 8 | Sand 5 | 35.0[(a)] | 29.5[(a)] |
| 9 | Clay 5 Bottom | 38.1 | 7.8 |
| 10 | Sand 6 | 35.0 | 29.5 |
| 11 | Clay 7 and 9<br>Sand 8 and 10 | 37.9 | 13.2 |

(a) Only one test performed – used mean value for Sand 6
Data Source: Subsection 2.4.12, Table 2.4.12-10

**Table 2.4.12-C-6**
**Summary of Model Boundary Conditions**

| Feature | Boundary Type | Elevation and General Location of Boundary |
|---|---|---|
| Linn Lake | Dirichlet (Type 1) – Constant Head | 10 ft – East of VCS site |
| Groundwater Flow Lines Model layers 2, 4, 6, 8, and 10 | Neuman (Type 2)- No Flow Boundary | Portions of the north and south model boundary – parallel to groundwater flow direction |
| Clay layers Model layers 1,3,5,7,9, and 11 | Neuman (Type 2)- No Flow Boundary | The no flow boundary condition was assigned to the perimeter of all clay layers, since the flow in these layers is primarily vertical |
| Recharge | Cauchy (Type 3) – Recharge | Uppermost active layer of the model |
| Evapotranspiration | Cauchy (Type 3) – ET | Layer 1 of the model |
| Victoria Barge Canal[a] | Cauchy (Type 3) – River | 0 ft (sea level canal) Eastern side of model domain |
| Guadalupe River[b] | Cauchy (Type 3) – River | 20 to 5 ft Eastern side of model domain |
| San Antonio River[b] | Cauchy (Type 3) – River | 62 to 5 ft Western and southern side of the model domain |
| Coleto Creek[b] | Cauchy (Type 3) – River | 72 to 19 ft North side of model domain |
| Black Bayou | Cauchy (Type 3) – River | 27 to 10 ft East of VCS site |
| Downgradient Seeps | Cauchy (Type 3) – Drain | 1 ft above bottom of drain cell East and north of VCS site |
| Kuy Creek | Cauchy (Type 3) – Drain | 1 ft above bottom of drain cell West and south of VCS site |
| Dry Kuy Creek | Cauchy (Type 3) – Drain | 1 ft above bottom of drain cell South of VCS site |
| Regional Groundwater Flow | Cauchy (Type 3) – General Head Boundary | Layers 4, 6, 7, 8, 9, and 10 (Refer to text for elevations) |

(a) Reference 2.4.12-31
(b) Reference 2.4.12-34

**Table 2.4.12-C-7 (Sheet 1 of 2)**
**Comparison of Simulated and Measured Heads**

| Well Name | Observed Head - $h_{obs}$ (ft NAVD 88) | Simulated Head - $h_{sim}$ (ft NAVD 88) | Residual Head ($h_{obs}$-$h_{sim}$) | Absolute Residual Head $\lvert h_{obs}-h_{sim} \rvert$ |
|---|---|---|---|---|
| 0W-10U | 22.27 | 29.93 | -7.66 | 7.66 |
| 7923601 | 68.91 | 74.00 | -5.09 | 5.09 |
| 7924102 | 48.90 | 47.77 | 1.13 | 1.13 |
| 7924702 | 58.44 | 59.11 | -0.67 | 0.67 |
| OW-01L | 30.00 | 25.91 | 4.09 | 4.09 |
| OW-01U | 30.73 | 30.02 | 0.71 | 0.71 |
| OW-02L | 24.31 | 23.96 | 0.35 | 0.35 |
| OW-02U | 24.55 | 28.22 | -3.67 | 3.67 |
| OW-03L | 19.03 | 22.46 | -3.43 | 3.43 |
| OW-04L | 22.62 | 23.96 | -1.34 | 1.34 |
| OW-04U | 23.59 | 27.82 | -4.23 | 4.23 |
| OW-05L | 25.61 | 25.69 | -0.09 | 0.09 |
| OW-05U | 26.07 | 29.58 | -3.51 | 3.51 |
| OW-06L | 26.19 | 26.23 | -0.04 | 0.04 |
| OW-06U | 26.35 | 30.06 | -3.71 | 3.71 |
| OW-07L | 19.62 | 24.17 | -4.54 | 4.54 |
| OW-07U | 19.91 | 28.45 | -8.55 | 8.55 |
| OW-08L | 32.54 | 30.70 | 1.84 | 1.84 |
| OW-08U | 36.02 | 31.71 | 4.31 | 4.31 |
| OW-09L | 27.17 | 26.25 | 0.92 | 0.92 |
| OW-09U | 26.93 | 30.30 | -3.37 | 3.37 |
| OW-10L | 23.48 | 26.20 | -2.72 | 2.72 |
| OW-2150L | 33.22 | 31.10 | 2.12 | 2.12 |
| OW-2150U | 44.85 | 34.48 | 10.37 | 10.37 |
| OW-2169L | 35.45 | 31.08 | 4.37 | 4.37 |
| OW-2169U | 41.92 | 34.24 | 7.68 | 7.68 |
| OW-2181L | 35.64 | 30.97 | 4.67 | 4.67 |
| OW-2181U | 41.62 | 34.17 | 7.45 | 7.45 |
| OW-2185L | 34.12 | 30.07 | 4.05 | 4.05 |
| OW-2185U | 38.30 | 33.66 | 4.64 | 4.64 |
| OW-2253L | 31.88 | 30.31 | 1.57 | 1.57 |
| OW-2253U | 45.40 | 33.79 | 11.61 | 11.61 |
| OW-2269L | 32.03 | 30.29 | 1.74 | 1.74 |
| OW-2269U | 34.03 | 30.17 | 3.86 | 3.86 |
| OW-2284L | 33.63 | 29.84 | 3.79 | 3.79 |
| OW-2284U | 42.75 | 33.52 | 9.23 | 9.23 |
| OW-2301L | 36.75 | 33.49 | 3.27 | 3.27 |
| OW-2301U | 49.25 | 36.86 | 12.39 | 12.39 |
| OW-2302L | 35.56 | 32.10 | 3.45 | 3.45 |
| OW-2302U | 37.30 | 33.36 | 3.94 | 3.94 |
| OW-2304L | 26.19 | 25.00 | 1.19 | 1.19 |

**Table 2.4.12-C-7 (Sheet 2 of 2)**
**Comparison of Simulated and Measured Heads**

| Well Name | Observed Head - $h_{obs}$ (ft NAVD 88) | Simulated Head - $h_{sim}$ (ft NAVD 88) | Residual Head ($h_{obs}$-$h_{sim}$) | Absolute Residual Head $\lvert h_{obs}-h_{sim} \rvert$ |
|---|---|---|---|---|
| OW-2304U | 34.12 | 26.01 | 8.12 | 8.12 |
| OW-2307L | 24.57 | 27.17 | -2.61 | 2.61 |
| OW-2307U | 31.39 | 31.22 | 0.17 | 0.17 |
| OW-2319L | 32.87 | 28.71 | 4.16 | 4.16 |
| OW-2319U | 33.95 | 28.76 | 5.19 | 5.19 |
| OW-2320L | 28.73 | 25.78 | 2.95 | 2.95 |
| OW-2320U | 27.75 | 25.36 | 2.39 | 2.39 |
| OW-2321L | 20.23 | 23.24 | -3.01 | 3.01 |
| OW-2321U | 20.40 | 22.60 | -2.20 | 2.20 |
| OW-2324L | 12.28 | 20.95 | -8.67 | 8.67 |
| OW-2324U | 12.74 | 20.49 | -7.75 | 7.75 |
| OW-2348L | 11.14 | 15.18 | -4.04 | 4.04 |
| OW-2348U | 10.91 | 14.90 | -3.99 | 3.99 |
| OW-2352L | 18.86 | 19.92 | -1.06 | 1.06 |
| OW-2352U | 18.83 | 18.94 | -0.11 | 0.11 |
| OW-2359L1 | 22.94 | 25.83 | -2.89 | 2.89 |
| OW-2359U1 | 22.94 | 25.59 | -2.65 | 2.65 |

**Table 2.4.12-C-8**
**Estimated Cooling Basin Seepage**

| Flow Component | Pre-Construction (gpm) | Post-Construction (gpm) | Change[(a)] (gpm) |
|---|---|---|---|
| Cooling Basin | 0 | **3930** | +3930 |
| Evapotranspiration | **(880)** | **(3770)** | +2890 |
| Kuy Creek | 0 | **(220)** | +220 |
| Dry Kuy Creek | 0 | **(460)** | +460 |
| Downgradient Drains | 0 | **(310)** | +310 |
| Black Bayou and Linn Lake | **(130)** | **(130)** | 0 |
| Victoria Barge Canal | **(16,240)** | **(16,520)** | +280 |
| Guadalupe River | **7510** | **7510** | 0 |
| San Antonio River | **(940)** | **(1110)** | +170 |

**(RED)** numbers indicate flow out of the model or base flow to creeks and rivers.
**BLUE** numbers indicate flow into the model – surface water inflow to groundwater.
Rates rounded to the nearest 10 gpm.

(a) "+" indicates an increase in flow from pre- to post-construction conditions and a "–" indicates a decrease.

| Flow Mass Balance | Pre-Construction (%) | Post-Construction (%) |
|---|---|---|
| Overall Flow Discrepancy | 0.04 | 0.15 |

**Table 2.4.12-C-9**
**Cooling Basin Seepage Sensitivity Analysis**

| Case | Cooling Basin Seepage Rate (gpm) | Change from Base Rate (gpm) |
|---|---|---|
| Base case Cooling Basin seepage | 3930 | 0 |
| River Boundary Conductance decreased 10x | 3360 | -570 |
| Layer 1 Clay hydraulic conductivity increased 10x | 4010 | +80 |

Rates rounded to the nearest 10 gpm.

**Table 2.4.12-C-10**
**Summary of Predictive Dewatering Simulations**

| Dewatering Scenario | Pumping Rate (gpm) |
|---|---|
| 1. Cooling Basin Empty – Full Site Dewatering | 990 |
| 2. Cooling Basin Full – Full Site Dewatering | 1840 |

Simulated pumping rates rounded to the nearest 10 gpm.

**Table 2.4.12-C-11**
**Summary of Particle Tracking Analysis**

| Scenario | Minimum Travel Time days (years) | Approximate Distance (ft) |
|---|---|---|
| 1- No Pumping | 41,000 (110) | 14,000 |
| 2- Northern Domestic Well pumping 50 gpm | 41,000 (110) | 14,000 |
| 3 – Western Domestic Well pumping 50 gpm | 41,000 (110) | 14,000 |
| 4 – Eastern Domestic Well pumping 50 gpm | 41,000 (110) | 14,000 |

Travel time in days reported to the nearest 1000 days, travel time in years reported to the nearest 5 years, and distance reported to the nearest 500 feet.